

**SILICON NITRIDE/SILICON NITRIDE
WHISKER-REINFORCED COMPOSITES**

Daniel Muscat

Department of Mining and Metallurgical Engineering
McGill University
Montreal, Canada.

August 1990

A Thesis submitted to the Faculty of
Graduate Studies and Research
in partial fulfillment of the
requirements for the degree of
Master of Engineering

D. Muscat, 1990.

To my Mother and Father.....

ABSTRACT

One of the major setbacks of ceramic materials is their inherent brittle nature which often leads to catastrophic failure, especially under impact and tensile stress conditions. Whisker-reinforcement of ceramic matrices has been shown to be an effective way of increasing toughness. However, the hot-pressing techniques being used at present are expensive. Si_3N_4 is a major contender for high temperature application, mainly due to its excellent mechanical, chemical and thermal properties.

In this work Si_3N_4 whiskers have been incorporated into a Si_3N_4 matrix and densified using pressureless sintering. An isotropic distribution of whiskers in the starting powder was seen to inhibit shrinkage of the bulk material as a result of whisker bridging.

An extrusion process was developed to align the whiskers such that they do not impinge on one another. This was done using a water soluble, cellulose based plasticizer. The process was sensitive to water content and mixing. Entrapped air caused problems in the extrudate, resulting in misaligned areas in the microstructure. Relative densities of 94.5% were obtained for composites having 15% whiskers. The toughness of this material was measured to be $13.5\text{MPa}\cdot\text{m}^{1/2}$ in the direction perpendicular to the direction of extrusion.

RÉSUMÉ

L'un des principaux désavantages des céramiques est leur nature fragile qui mène souvent à une défaillance soudaine. Le renforcement par barbes (*whisker-reinforcement*) des matrices de céramiques est une façon éprouvée d'augmenter leur ténacité. Toutefois, les techniques de compression à chaud présentement utilisées sont onéreuses. Les excellentes propriétés mécaniques, chimiques et thermiques de Si_3N_4 en font un matériau de choix pour les applications à haute température.

Dans cette étude, des barbes de Si_3N_4 ont été incorporées dans une matrice de Si_3N_4 et densifiées par frittage à pression atmosphérique. Il a été possible de démontrer qu'une distribution isotropique des barbes dans la poudre au départ résulte dans la formation de ponts et empêche un rétrécissement de volume.

Un procédé d'extrusion a été développé afin d'aligner les barbes de façon à ce qu'elles ne se heurtent pas entre elles. Ceci a été accompli à l'aide d'un plastifiant à base de cellulose, soluble dans l'eau. Ce procédé s'est avéré sensible à la quantité d'eau ainsi qu'à la façon d'effectuer le mélange. L'air emprisonné dans le produit d'extrusion a causé des problèmes résultant en zones non-alignées dans la microstructure.

Des densités relatives de 94.5% ont été obtenues pour des composites ayant une teneur de 15% de barbes. La ténacité de ce matériau a été évaluée à $13.5\text{MPa}\cdot\text{m}^{1/2}$ perpendiculairement à la direction d'extrusion.

ACKNOWLEDGEMENTS

I would like to express my sincere gratitude to Prof. R.A.L. Drew for his supervision and encouragement throughout the course of this thesis.

I would also like to thank Prof. M.D. Pugh for his advice and suggestions, as well as for his reviewing of the thesis.

Special thanks goes to Dr. K. Shanker for his suggestions and expert opinion, and also for proof reading the thesis.

I would like to thank Mr. M. Knopfel and all machine shop personnel for being so helpful in the workshop.

I would also like to thank Prof. D.C. Gray, director of the Pulp and Paper centre at McGill University, for providing me with information and references.

Finally I would like to thank Mr. S. Grenier for translating the abstract into French, Mr. M. Xun for assisting me in reprinting the micrographs and all my other colleagues in the ceramics group for their contribution, by way of help and support, to this work.

TABLE OF CONTENTS

ABSTRACT	iii
RESUME	iv
ACKNOWLEDGEMENTS	v
TABLE OF CONTENTS	vi
LIST OF FIGURES	ix
LIST OF TABLES	xii
1. INTRODUCTION	1
2. BACKGROUND INFORMATION & LITERATURE REVIEW	5
2.1 SILICON NITRIDE	6
2.1.1 FORMATION, STRUCTURE AND PROPERTIES	6
2.1.2 FABRICATION OF Si_3N_4	9
2.1.2.1 Densification of Ceramics	9
2.1.2.2 Densification of Si_3N_4	11
2.1.3 FABRICATION PROCESSES OF Si_3N_4	15
2.1.3.1 Reaction Bonded Silicon Nitride	15
2.1.3.2 Sintered Si_3N_4	16
2.2 THEORETICAL ASPECTS OF FIBRE REINFORCEMENT	18
2.2.1 TOUGHENING MECHANISMS IN WHISKER/FIBRE REINFORCED SYSTEMS	18
2.3 CONTINUOUS FIBRE-REINFORCED CERAMIC COMPOSITE SYSTEMS	21

2.4 WHISKER-REINFORCED CERAMIC COMPOSITE SYSTEMS	22
2.4.1 SELECTION OF RAW MATERIAL	22
2.4.1.1 The Matrix	22
2.4.1.2 The Whiskers	23
2.4.1.3 The Liquid Phase	23
2.4.2 PROCESSING TECHNOLOGY	24
2.4.2.1 Mixing and Dispersion	25
2.4.2.2 Consolidation of Whisker Composites	30
2.4.2.3 Sintering	31
2.4.3 MECHANICAL PROPERTIES	34
2.4.4 HIGH TEMPERATURE PROPERTIES	36
2.5 SUMMARY	37
3. OBJECTIVES	39
4. EXPERIMENTAL PROCEDURE	40
4.1 RAW MATERIAL CHARACTERIZATION	40
4.2 POWDER DISPERSION AND MIXING	42
4.2.1 ATTRITION MILLING/ULTRASONIC DISPERSION	42
4.2.2 pH ADJUSTMENT	43
4.3 DRYING AND GRANULATING	44
4.4 FABRICATION OF SAMPLES	45
4.4.1 PRESSING	45
4.4.2 EXTRUSION	46

4.5 SINTERING	48
4.6 SAMPLE PREPARATION FOR MECHANICAL TESTING	49
4.6.1 MODULUS OF RUPTURE	50
4.6.2 TOUGHNESS	50
4.7 PREPARATION FOR MICROSCOPICAL EXAMINATION	51
5. RESULTS & DISCUSSION	53
5.1 PRESSING	53
5.1.1 POWDER/WHISKER DISPERSION	53
5.1.2 MICROSTRUCTURAL ANALYSIS AND DENSIFICATION	55
5.1.3 WHISKER CHARACTERIZATION	62
5.1.4 MECHANICAL PROPERTIES	64
5.2 EXTRUSION	66
5.2.1 SAMPLE FABRICATION	68
5.2.2 SHRINKAGE	74
5.2.3 MICROSTRUCTURAL EXAMINATION AND DENSIFICATION	76
5.2.4 MECHANICAL PROPERTIES	85
6. CONCLUSIONS	90
7. SUGGESTED FUTURE WORK	92
8. REFERENCES	93

LIST OF FIGURES

1.1: World market for Advanced Ceramics, 1988.	2
2.1: The structural formulae for: (a) α -Si ₃ N ₄ ; (b) β -Si ₃ N ₄ .	7
2.2: Mass transport paths during sintering.	10
2.3: Liquid-phase sintering.	11
2.4: Liquid-phase sintering of Si ₃ N ₄ .	12
2.5: The α - β transformation.	13
2.6: The SiAlON PHASE DIAGRAM AT 1700°C	14
2.7: The Y-SiAlON system.	15
2.8: (a) Crack arrest, (b) Crack deflection.	20
2.9: The electrostatic double layer.	27
2.10: Steric repulsion.	28
2.11: The effect of whisker content on density for pressureless sintered specimens.	32
2.12: Density increase using various sintering methods.	34
4.1: UBE Si ₃ N ₄ whiskers.	41
4.2: Processing route for attrition milling whiskers and powder.	43
4.3: Processing of whiskers and powder using pH adjustment.	44
4.4: Processing route for fabricating pressed bars.	46
4.5: Processing route for fabricating extruded samples.	47
4.6: A schematic of the sintering furnace.	49
4.7: 4-point testing of ceramic samples.	50

5.1: Relative green density vs. whisker content.	54
5.2: Relative sintered densities vs. whisker content.	55
5.3: Fractured surface of green compact (15% whiskers).	56
5.4: Fractured surface of Si_3N_4 with 30% whisker content.	57
5.5: X-ray diffraction of sintered $\beta\text{-Si}_3\text{N}_4$ (30% whiskers), compared to a standard.	58
5.6: Schematic of the whisker bridging effect which jams densification, a) vapour-liquid-solid growth, and b) shrinking of entrapped powder.	59
5.7: Polished surface of Si_3N_4 with 30% whiskers (NaOH etch).	60
5.8: Polished surface of Si_3N_4 with 15% whisker content.	60
5.9: Polished surface of Si_3N_4 with 5% whiskers (NaOH etch).	61
5.10: Sample of whiskers separated from the as-received batch.	63
5.11: Whiskers after 2 hours of attrition milling (Aspect Ratio=5-35).	64
5.12: M.O.R. values vs. whisker content.	65
5.13: The HPC molecule.	67
5.14: Schematic of polymer/whisker interaction.	67
5.15: Sintered density vs. water content in extrudate.	70
5.16: The inclusion of a spider in the nozzle.	71
5.17: Fracture surface of green compact after burn-out (no whiskers).	72
5.18: Fracture surface of green compact after burn-out extruded through mesh into a vacuum (15% whiskers).	73
5.19: Fracture surface of green compact extruded under standard conditions, after burn-out (15% whiskers).	73
5.20: Fracture surface of green extrudate mixed using mechanical	74

mixing, after burn-out (15% whiskers).

5.21: Isotropic shrinkage of pressed samples versus anisotropic shrinkage of extruded samples containing whiskers.	75
5.22: Green extrudate showing whisker alignment (15% whiskers).	77
5.23: Polished sintered extrudated showing alignment (NaOH etch).	77
5.24: Microstructure of monolithic Si_3N_4 .	78
5.25: Sintered extruded sample showing preferred grain growth.	79
5.26: Schematic of the sintering of aligned whisker composites.	80
5.27: A region of low density, probably a white spot in a polished sintered extrudate (15% whiskers), etched with HF.	81
5.28: fracture surface of C.I.P. sample, showing misalignment.	82
5.29: optical micrograph of agglomerates remaining in the paste.	83
5.30: The agglomerates after being broken up by shearing.	84
5.31: optical micrograph of the paste after being mixed mechanically.	84
5.32: Fracture origin of M.O.R. test sample.	85
5.33: Optical micrograph of a Vicker's indent to measure toughness.	86
5.34: Intergranular fracture along the reinforcement.	88
5.35: Transgranular fracture across reinforcement.	88
5.36: Branching, and deflection of the crack.	89

LIST OF TABLES

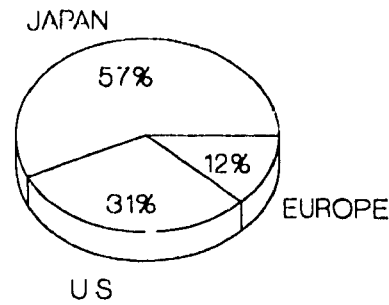
Table 2.1: Properties of Si_3N_4 ceramics.	8
Table 2.2: Densities for slip cast and CIP specimens.	33
Table 2.3: Mechanical properties of Hot-Pressed $\text{Al}_2\text{O}_3/\text{SiC}_w$ composites.	35
Table 2.4: Mechanical properties of various $\text{Si}_3\text{N}_4/\text{SiC}_w$ composites.	36
Table 4.1: Specification of starting powder and whiskers.	40
Table 4.2: Composition of starting powder mixture.	42
Table 5.1: Comparison of size and A.R. for whiskers before and after sintering.	78
Table 5.2: Toughness values for a 15% whisker-reinforced extrudate.	87

1. INTRODUCTION

Over the past 25 years, there has been an ever increasing interest in engineering ceramics as new materials with outstanding properties. The range of materials that may be classified as ceramics is so vast, there is no one definition which can be used to encompass them all. In addition, the application of these materials in engineering is probably just as vast. These new ceramic materials have to be distinguished from their traditional counterparts, such as clays, porcelains and glass.

Advanced ceramics are materials designed for specific applications, with the greatest interest being for electronic and structural applications⁽¹⁾. Currently, electronic applications, by far, dominate the world market, i.e. 84% of the total volume or higher⁽²⁾, with structural applications sharing the remainder. Areas in electronics include semi-conductors, super-conductors, packaging materials such as substrates and capacitors, ferrites, piezoelectrics, sensors etc.. Structural ceramic applications include heat engines such as turbines and combustion engines, cutting tools, mining and drilling equipment, sludge pump components, etc.. Other areas of science developing uses for ceramic materials are in dentistry and bone implants.

Total world market prediction vary somewhat from one study to another but what is certain is that there will be an increasing demand for these materials within the next 10-20 years. The market in 1988 was estimated at \$12 billion by Kline and Co.(Fig 1.1), with predictions reaching \$24.5 billion by the year 1995 (according to Freedonia Group Inc.)⁽²⁾.



Total=\$12 billion

Fig. 1.1: World market for Advanced Ceramics, 1988⁽²⁾.

Advanced structural ceramics provide properties such as good strength (even at temperature where metallic counterparts begin to deteriorate), good wear and chemical resistance, high thermal conductivity, and good thermal properties such as high temperature chemical stability and thermal shock resistance. Examples of such ceramic materials are those based on: silicon nitride (Si_3N_4), silicon carbide (SiC), alumina (Al_2O_3) and zirconia (ZrO_2).

Because of their covalent nature, ceramic materials are inherently brittle. This means that if a crack initiates in the material, it will propagate to failure in a catastrophic fashion. A crack may initiate at a point where there is a stress concentration, and in brittle structural ceramics these are generally flaws in the form of pores, or inclusions. These flaws are mostly associated with processing^(3,4). Due to this factor of uncertainty, the strengths of these brittle materials are measured using a statistical approach (the occurrence of flaws is described by a statistical

distribution). However, this is not enough to convince mechanical engineers to design with ceramics; although it may seem statistically safe to apply a structural ceramic in a critical application, there will always be a chance of early failure in a catastrophic manner. The answer to this problem is to improve the fracture toughness of the material, i.e. its K_{Ic} . A possible approach to this is to form a composite with the material. This philosophy has been applied successfully in polymer and metal matrices^(5,6), although in these cases improving the strength and stiffness was the primary objective. Nevertheless, the idea of incorporating a second phase into ceramic matrices to inhibit crack propagation has been investigated, and in some instances has proved very successful, as in, for example, glass fibre-reinforced concrete⁽⁷⁾.

A composite material is one that contains at least two phases. Generally one phase is stronger than the other, to give a *reinforced composite*. Reinforcement may be in the form of fibres, particulate or laminates. Fibres may be *continuous* or *discontinuous*. A fibre is continuous when a change in its length does not alter the properties of the matrix material; usually these fibres have a length comparable to the dimension along the direction which they reinforce. Discontinuous fibres may be short fibres (chopped continuous) or *whiskers*. The latter are elongated single crystals having strengths approaching the bond strength of the material with sub-micron diameters and aspect ratios (l/d) ranging from 10-50.

There are a number of commercially available fibres on the market, and many of these have already been investigated in combination with various ceramic matrices; the most common one being the carbon fibre⁽⁸⁾. This is then followed by SiC⁽⁹⁾ fibres

and some work has also been carried out on Al_2O_3 fibres⁽¹⁰⁾. These fibres have been incorporated in matrices such as SiC ⁽¹¹⁾, Al_2O_3 ⁽¹²⁾, Si_3N_4 ⁽¹³⁾ and glass ceramics⁽¹⁴⁾. Commercially available whiskers are mostly of SiC , although whiskers of other materials, such as Si_3N_4 , have been produced. SiC whiskers have been successfully incorporated into Al_2O_3 and Si_3N_4 matrices. This work will be reviewed in some detail in Chapter 2.

Thus the need to produce reinforced ceramic composites with increased toughness is clear, and this work is concerned with the processing of such a material.

2. BACKGROUND INFORMATION & LITERATURE REVIEW

During the past 10 years, ceramic composites have stirred up much excitement in materials science, mostly because of their potential resulting from their unparalleled properties. Thus there has been tremendous effort in trying to develop the science of ceramic matrix composites. As a result, a large quantity of data has been generated, and an understanding of the fundamentals regarding processing and fabrication has already been established^(15,16), although even here new developments occur frequently. The properties obtained for these new materials have been documented by a number of authors^(17,18,19) using various classification methods. Current fundamental knowledge of factors that determine mechanical properties of ceramic composites, and ways of improving them, has also been the topic of numerous publications^(20,21,22).

The aim of this chapter is to review in more detail, the work carried out on this subject to date, with special reference to whisker reinforcement of ceramics. The more important areas of this science, as well as the current research interest, will be emphasized, with regard to the present work. But before moving on to composites, a brief review of the basic concepts of ceramics and the matrix material, namely silicon nitride (Si_3N_4), will be presented.

2.1 SILICON NITRIDE

To fully understand the objectives of this work, and the mechanisms involved, a thorough understanding of the matrix material is necessary. The following section summarises the current knowledge of the material.

2.1.1 FORMATION, STRUCTURE AND PROPERTIES

Si_3N_4 does not occur naturally on the Earth's surface and is synthetically formed by the combination of silicon and nitrogen. This is done either by heating silicon powder in nitrogen, or through the carbothermal reduction of silica in nitrogen, or by the ammoniolytic of silicon tetrachloride. These methods have been reviewed elsewhere⁽²³⁾.

Si_3N_4 is found in two crystalline forms, α and β ⁽²⁴⁾. Both have hexagonal structures, but with differing lattice parameters in the c -axis; that of α being about twice that of β ⁽²⁵⁾. This is due to differences in the stacking sequence of the planes. Whereas β consists of Si_6N_8 layers, alternating in the sequence ABAB, α consists of $\text{Si}_{12}\text{N}_{16}$ planes in a sequence ABCD, where CD are mirror inverted layers of AB. This accounts for the α lattice distance being twice that of the β crystal.

It was proposed that the α phase (Fig. 2.1a) is further stabilized by the presence of oxygen in the structure⁽²⁶⁾, to form an oxynitride with a chemical formula $\text{Si}_{11.4}\text{N}_{15}\text{O}_{0.3}$. However this observation has been questioned^(27,28,29) and current

consensus is that α - Si_3N_4 does not necessarily require oxygen for structural stability. The β -phase is derived from the structure based on that of phenacite (Be_2SiO_4), as shown in Fig. 2.1b, where the beryllium atoms are replaced by silicon, and the oxygen atoms replaced by nitrogen⁽³⁰⁾.

Both phases may be synthesised concurrently over a wide temperature range⁽³¹⁾, however, the α phase becomes increasingly unstable, with respect to β , at higher temperatures, and it is now widely accepted that α is a low temperature, metastable phase ($<1500^\circ\text{C}$), whereas β is stable at all temperatures⁽³²⁾.

Due to the rigid nature and directionality of the covalent bond, Si_3N_4 is a hard, strong material with a high decomposition temperature. Pauling⁽³³⁾ estimated the

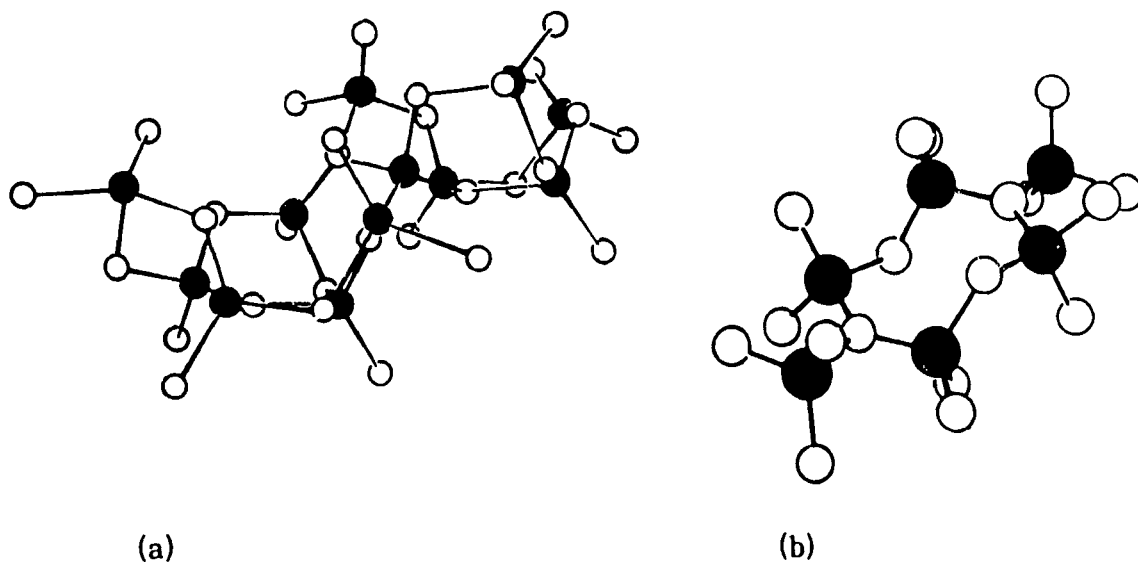


Fig. 2.1: The Structural formulae for: (a) α - Si_3N_4 ; (b) β - Si_3N_4 .

bonding of Si_3N_4 to be ~70% covalent. Like most ceramics, it is also brittle. It is light, has a low thermal expansion coefficient and is a good conductor of heat. The combination of these properties make Si_3N_4 an excellent material for high temperature applications. Dense Si_3N_4 is transparent, but due to the presence of impurities like Fe, Ca and Al the material appears grey. It is inert to most corrosive environments, except hydrofluoric acid and molten alkali salts. Table 2.1 compares some of the properties of dense Si_3N_4 to another commercially available material known as *reaction-bonded silicon nitride*, the fabrication of which will be described in 2.1.3.1.

Table 2.1: Properties of Si_3N_4 ceramics⁽³⁴⁾.

PROPERTIES	DENSE Si_3N_4	RBSN
CRYSTAL STRUCTURE	α : c/a=0.70 β : c/a=0.37	
DECOMPOSITION TEMPERATURE ($^{\circ}\text{C}$)	1920	
THEORETICAL DENSITY (g/cm^3)	α = 3.168-3.188 β = 3.19-3.202	
RELATIVE DENSITY	90-100% th.	70-88% th.
THERMAL EXP. COEFF. ($/10^6$ $^{\circ}\text{C}$)	2.9-3.6	
THERMAL COND. (W/mK)	15-50	4-30
SPECIFIC HEAT (J/kg $^{\circ}\text{C}$)	700	
MICROHARDNESS (VICKERS, GPa)	16-22	
YOUNG'S MOD.(GPa)	300-330	120-220
FLEXURAL STRENGTH (MPa)	400-950	150-350
FRACTURE TOUGHNESS ($\text{MPa}\cdot\text{m}^{1/2}$)	3.4-8.2	1.5-2.8

The mechanical, chemical and electrical properties depend strongly on the extent of densification of the bulk material. This is a challenging aspect in the fabrication of the material. The following section reviews the mechanisms involved in doing this.

2.1.2 FABRICATION OF Si_3N_4

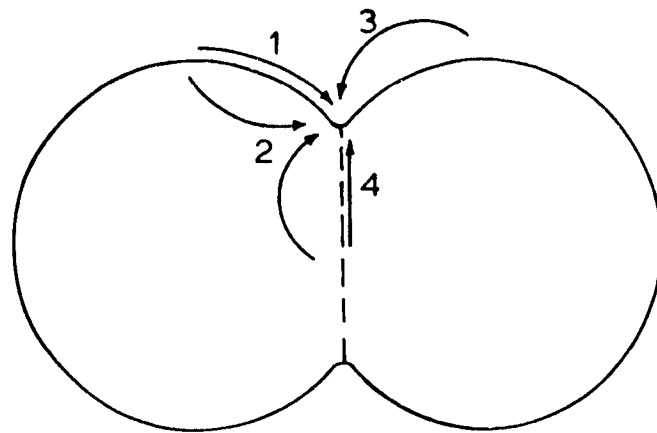
Prior to reviewing the kinetics by which Si_3N_4 densifies, a brief description of densification theory in ceramic materials will be presented.

2.1.2.1 Densification of Ceramics

A ceramic body develops useful mechanical properties after *sintering* a powder compact, or *green body*. Sintering is a heat-treatment process whereby particulate material (green body) is heated to a temperature high enough for material transport to take place. A green body typically contains 25-60% porosity, and the powder is loosely held together by weak van der Waal forces and mechanical interlocking. Upon sintering, there is a thermodynamic driving force for the compact to reduce its overall surface area. This is done by the elimination of pores, i.e. the change from high surface free energy solid-vapour interfaces to the lower solid-solid interfaces (this results in an overall shrinkage of the body)⁽³⁵⁾. It thus follows that the smaller the particle size of the powder, the higher the driving force for densification.

Material transport takes place in a number of ways, either by solid-state

diffusion through the lattice, the surface or the grain boundaries, or via a vapour phase (evaporation-condensation) along the grain surfaces (Fig 2.2)⁽³⁵⁾. Alternatively, it could occur via a liquid phase along the surface. For this to take place: there should be an appreciable amount of liquid phase present; the solid phase should be soluble to some extent in the liquid; and the liquid must wet the solid surfaces. This liquid phase is generally formed by additives which, upon heating, melt at a lower temperature than that required for solid-state diffusion to occur. The liquid thus wets the surface of particles, creating a capillary pressure between each interparticle spacing. This brings particles closer together as a result of a negative curvature that is present at the point of contact of two particles (Fig 2.3)⁽³⁵⁾. This liquid phase helps sintering in a number



1. Surface Diffusion
2. Bulk Diffusion
3. Vapour diffusion
4. Grain Boundary Diffusion

Fig. 2.2: Mass transport paths during sintering.

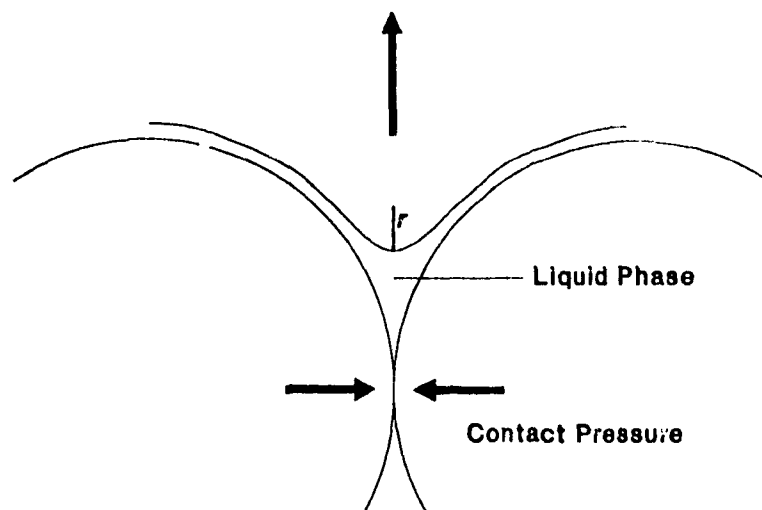


Fig. 2.3: Liquid-phase sintering.

of ways: it allows particle rearrangement by creep for more efficient packing and increases the rate of mass transport by solid-state diffusion (higher contact pressure), as well as by a solution-precipitation process through the liquid⁽³⁶⁾.

2.1.2.2 Densification of Si_3N_4

Due to the highly covalent nature and short interatomic distances of Si_3N_4 , densification by solid state diffusion is not a practical approach⁽³⁷⁾. Material transport is too slow for sintering to occur in a realistic time. In fact, it has been shown⁽³⁸⁾ that the self-diffusion coefficient (D) for Si in Si_3N_4 at 1900°C is only $1.5 \times 10^{-16} \text{ m}^2 \text{ s}^{-1}$. Therefore much work has been directed towards sintering in the presence of a liquid phase.

Liquid Phase Sintering of Si_3N_4

The liquid phase for Si_3N_4 is provided by sintering additives, mixed in with the starting powder. Upon heating, they react with the surface silica in the Si_3N_4 powder, to form silicate compounds, as shown in Fig. 2.4.

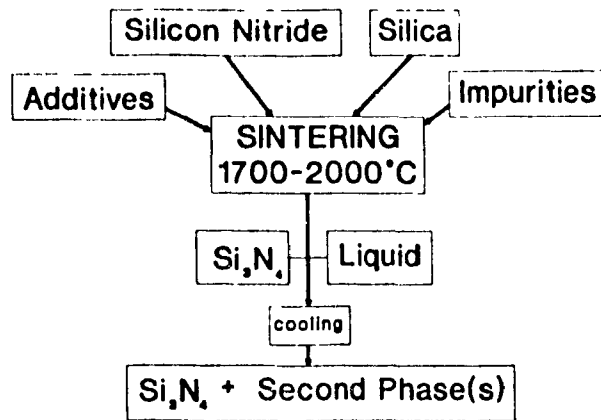


Fig. 2.4: Liquid-phase sintering of Si_3N_4 .

The Si_3N_4 and liquid phase combinations have been studied extensively, the more important additives being MgO , Y_2O_3 and AlN , with Al_2O_3 , forming the $Mg-Si-O-N$, $Y-Si-O-N$ ^(39,40) and $Si-Al-O-N$ ^(41,42) systems respectively. These systems will be briefly discussed later.

The α to β Transformation

The α to β transformation is a major step in the densification of Si_3N_4 . This step has almost always been observed in the presence of a liquid phase. As mentioned earlier, the liquid phase allows the Si_3N_4 to dissolve. This dissolution of nitrogen in a

silicate or oxynitride melt, favours the formation of the β phase by the solution-precipitation process^(43,44,45). Without the liquid phase, transformation would otherwise be too sluggish to proceed⁽⁴⁶⁾. The β crystals that precipitate tend to have an acicular structure^(43,47,48). Fig. 2.5 shows a schematic of this transformation.

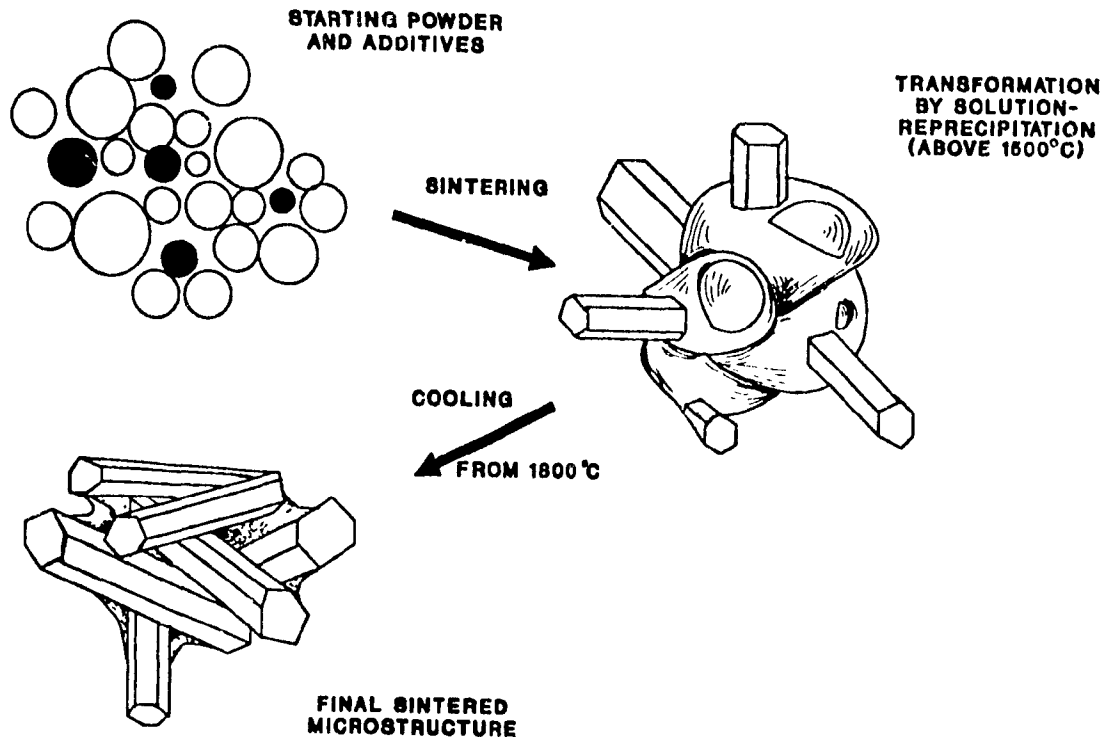


Fig. 2.5: The α - β transformation.

SIALON Ceramics

A major development of the liquid phase system was the simultaneous discovery of the Si-Al-O-N system (Fig. 2.6) by Jack et al.⁽⁴¹⁾ and Omayya et al.⁽⁴²⁾. In this

system the additives form an alloy with β Si_3N_4 by the substitution of aluminum and oxygen for silicon and nitrogen, respectively. This produces a solid-solution phase of the same crystal structure as β , and is termed β' -sialon. The additions may be in the form of Al_2O_3 , or a combination of Al_2O_3 and AlN . The addition of yttria to the system (Y-SiAlON, Fig. 2.7) provides a more extensive liquid region, thus allowing for liquid phase sintering to proceed more easily. Upon cooling, the liquid phase forms an yttrium sialon glass grain boundary phase⁽⁴⁹⁾. Depending on the composition, this may then be heat-treated to form a crystalline phase, such as yttrium aluminum garnet ($\text{Y}_3\text{Al}_2\text{O}_{12}$)⁽⁵⁰⁾. By doing so, the material may be engineered to be more creep resistant at temperatures as high as 1400°C ⁽⁵¹⁾.

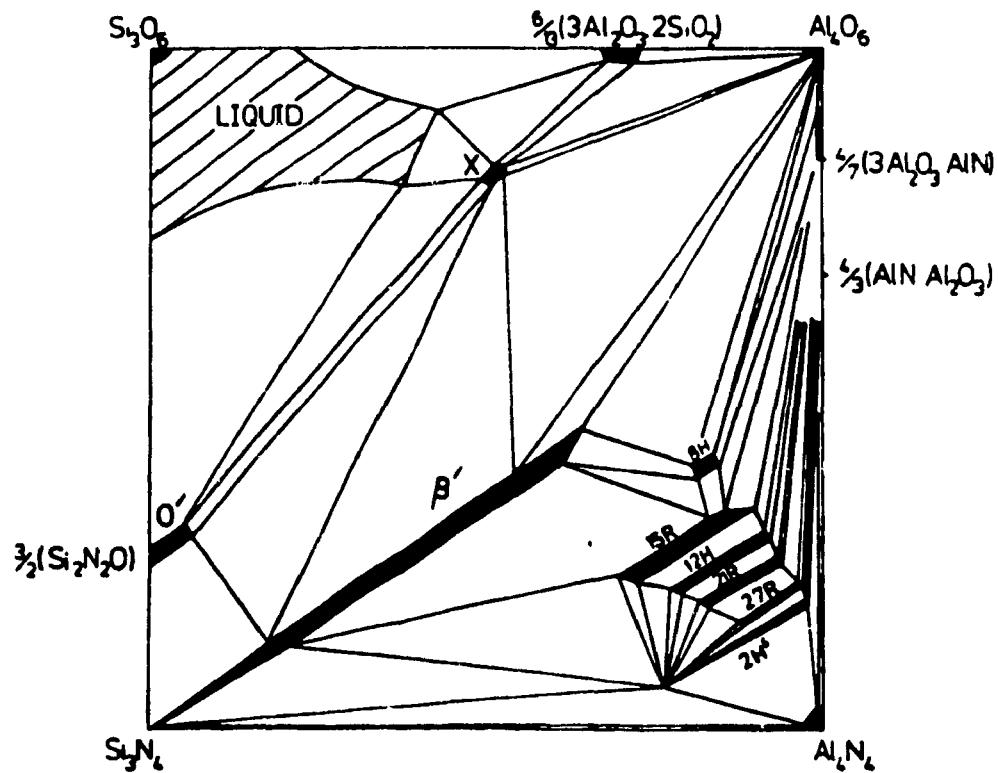


Fig. 2.6: The SiAlON phase diagram at 1700°C .

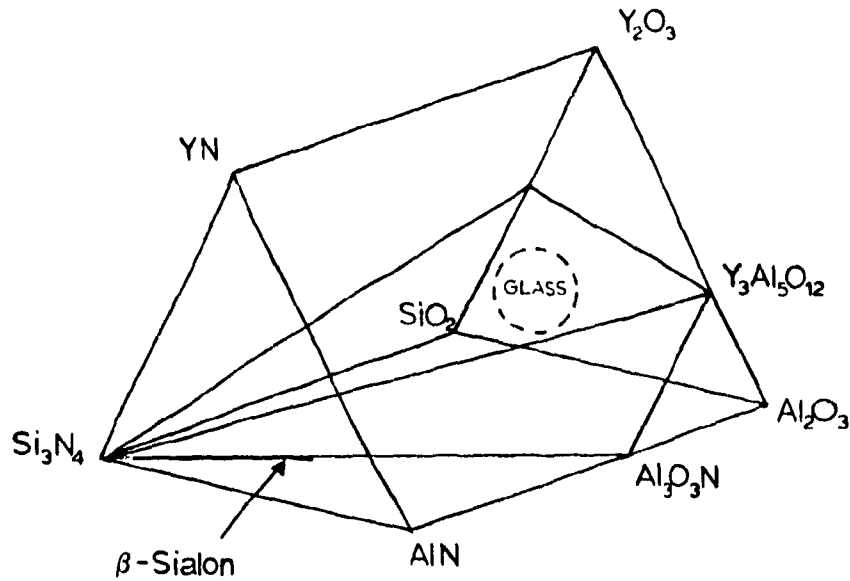


Fig. 2.7: The Y-SiAlON system.

2.1.3 FABRICATION PROCESSES OF Si_3N_4

As mentioned earlier, Si_3N_4 bodies are made by sintering a green powder compact. There are basically two routes that may be taken to do this. The first is the direct nitridation of a silicon powder compact, to form *reaction bonded silicon nitride* (RBSN), and the second involves the sintering of a Si_3N_4 powder compact using the application of pressure, be it external (hot-pressing) or by the presence of a liquid phase as described in 2.1.2.2 above, or both.

2.1.3.1 Reactor Bonded Silicon Nitride

This method provides a simple way of producing near net shape objects. The

starting material is a silicon powder compact which is first pre-sintered at low temperature. This provides sufficient strength for conventional machining of complex shapes. Nitridation then follows at temperatures of 1200-1450°C and can take up to several days for large components. The result is a porous matrix (at least 15% porosity) with the matrix being made up of 60-90% α - Si_3N_4 , and the remainder β . This process has been described in detail by Moulson⁽⁵²⁾, and further discussion is beyond the scope of this work.

2.1.3.2 Sintered Si_3N_4

Sintering of Si_3N_4 may be achieved either by using external pressure, or by using a liquid phase, or both, to speed up the diffusion processes. Two methods have been developed to do this: Pressing, which includes Hot-Pressing and Hot Isostatic Pressing (HIPping); and Sintering, which includes Pressureless sintering and Gas Pressure sintering.

Hot Pressing

This method uses the application of external pressure while sintering at about 1650-1750°C. The pressure is applied by using a graphite die, which is then rammed uniaxially, or by using gas pressure. Fully dense Si_3N_4 with good mechanical properties may be produced using this technique. However its major disadvantage is the high cost of equipment and the fact that only simple symmetrical shapes may be produced;

complex shapes require extensive diamond machining. It also promotes grain alignment in a plane perpendicular to the direction of the force. Because of these disadvantages, it is not considered a viable process for use in industry.

Hot Isostatic Pressing (HIP)

This method is similar to Hot Pressing in that it uses the application of pressure during sintering. However the difference is that the pressure is applied isostatically, thus allowing complex shaped objects to be manufactured. This requires that the object be encapsulated prior to sintering. The technique gives very uniform microstructures and material with very good properties. However it is an expensive process and is not very practical for production purposes.

Pressureless Sintering

The answer to producing a low cost, dense, complex-shaped Si_3N_4 article seems to be pressureless sintering. This method uses the capillary pressure created by the presence of the liquid phase as the driving force for fast diffusion. Furnace design is much simpler than that requiring external pressure. However in this technique it is important to have an ultra-fine starting powder to provide the thermodynamic driving force for densification, as explained in 2.1.2 above. A close control of the partial pressure of the reactants in the sintering atmosphere is necessary to avoid dissociation of the Si_3N_4 . This is achieved by the use of a nitrogen atmosphere, and a bed of loose Si_3N_4 and BN powder.

Gas Pressure Sintering

This method is a modification of pressureless sintering. The partial pressure of the nitrogen is increased above atmospheric. This enhances the densification process somewhat, and also prevents decomposition of the components being sintered. The sintering temperature can also be increased, and as a result, sintering times are reduced.

2.2 THEORETICAL ASPECTS OF FIBRE REINFORCEMENT

As previously mentioned, one of the main directions of research in ceramics is to improve the reliability of an advanced structural ceramic. There appears to be two approaches to this problem⁽²¹⁾. The first is to eliminate defects resulting from processing⁽³⁾, thus reducing the size and distribution of *critical flaws* which initiate failure. In this way, ceramic materials with high uniform flexural strengths and a high Weibull Modulus (a measure of reliability) are obtained. The second approach is to reinforce the matrix with fibres, and try to control the crack propagation, hence reducing the chances of catastrophic failure.

2.2.1 TOUGHENING MECHANISMS IN WHISKER/FIBRE REINFORCED SYSTEMS

The most complete discussion of the mechanisms involved in fibre reinforcement is given by Rice⁽⁵³⁾. The mechanisms most applicable to advanced ceramics are

summarized as follows:

a) Load Transfer

This is a fundamental concept in a composite material. The stress in the material is distributed equally amongst the fibres and the matrix, in proportion to the volume ratio between the two phases. The extent of toughening generally increases with the ratio E_f/E_m and the volume of fibres added (V_f).

b) Crack-Particle Interaction

i. Crack Impediment

This mechanism requires fibres which are more difficult to fracture than the matrix. This results in a crack bowing out between the fibres until it reaches a breakaway condition⁽⁵⁴⁾ as proposed in Lange's line tension model. Evans⁽⁵⁵⁾ further analysed fibre shape and orientation, deducing that maximum benefit of this mechanism is achieved when uniaxial fibres are aligned parallel with the principal stress.

The stresses arising due to a thermal expansion coefficient mismatch between fibre and particle could significantly affect the path of a crack. Cracks prefer to propagate normal to tensile stresses and parallel with compressive stresses. Thus it follows that a crack is attracted to a fibre in hydrostatic compression, provided the crack approaches the particle close enough for the stress to become effective. This is shown schematically in Fig. 2.8(a).

ii) Crack Deflection/Forking

Similarly as above, a reversed situation, that is having a fibre in hydrostatic tension, would make a crack deflect away from the fibre (Fig. 2.8(b)). A second mechanism resulting in a crack deflecting or forking is the orientation of preferred fracture surfaces such as grain boundaries or cleavage planes. This mechanism could be enhanced by providing oriented arrays of preferred paths, such as crystallographic oriented precipitates. Toughening is increased as a result of reduced stress intensity in the set of cracks, and increased fracture area.

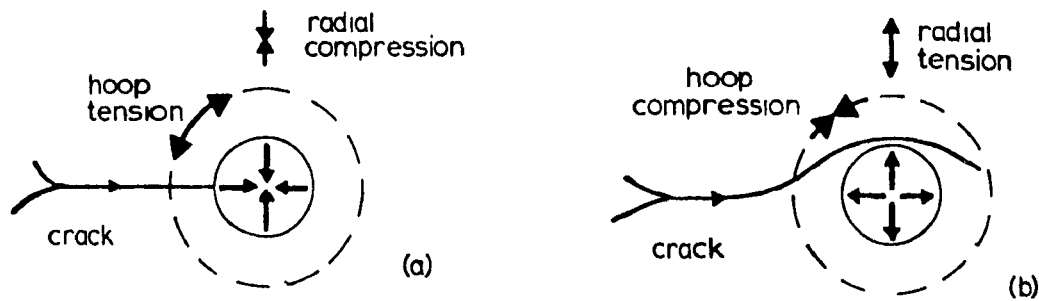


Fig. 2.8: (a) Crack arrest, (b) Crack deflection⁽⁵³⁾.

iii) Fibre Pullout

Fibre pullout will occur when the fibre has a high transverse fracture toughness, or when there is poor bonding between the fibre and the matrix. If pullout occurs, the effective fracture surface increases and thus increases the overall toughness. The nature of the fibre/matrix bond is very critical in achieving this type of toughening⁽⁵⁶⁾

and considerable efforts have been made to characterize these interfaces. Coatings that produce a weak fibre/matrix interface bond have now been developed to optimize this toughening mechanism⁽⁵⁷⁾.

c) Whisker Bridging

This mechanism is derived from strong whiskers which bridge the crack in the region behind the crack tip. In addition, whiskers further behind the crack tip fracture and/or may be pulled out of the matrix⁽⁵⁸⁾. Furthermore, in the case of aligned whiskers, the closure stress exerted by the bridging whiskers is the sum of the closure stresses exerted by each whisker in the bridging zone.

2.3 CONTINUOUS FIBRE-REINFORCED CERAMIC COMPOSITE SYSTEMS

The development of glass and carbon continuous fibres for polymer matrix applications brought about the birth of continuous fibre-reinforced ceramics⁽⁵⁹⁾. Today fibres of SiC, and to some extent Al₂O₃, have been successfully incorporated in matrices of SiC^(11,60), Si₃N₄^(13,61), Al₂O₃^(12,62), to mention but a few. A major area of development in these systems is the depositions of protective coating to inhibit severe degradation of the fibres, by interaction with the matrix material^(57,63). The extent of research carried out in this area of ceramic composites is too vast to be reviewed here, but further information can be obtained in the references given above.

2.4 WHISKER-REINFORCED CERAMIC COMPOSITE SYSTEMS

The area of whisker-reinforced composite materials is still highly active and information is being generated at a very fast rate. The interest in the field is clearly visible by the number of researchers working towards establishing the relevant science. However, it is apparent that there are certain areas which are being given particular attention. These may be summed up as follows:

- Choice of starting material, to ensure fast, and complete densification.
- Good dispersion of the whiskers and starting powder, including choice of method (pH control of slurry, dispersants, milling, etc.) thus eliminating flaws resulting from processing and hence maximizing the mechanical properties.
- To obtain densification using cheap methods such as pressureless sintering.
- To obtain improved high temperature properties.

The two most established systems being researched are the SiC whisker-reinforced Al_2O_3 matrix system ($\text{Al}_2\text{O}_3/\text{SiC}_w$), and the SiC whisker-reinforced Si_3N_4 matrix system ($\text{Si}_3\text{N}_4/\text{SiC}_w$). These will continually be referred to in this chapter.

2.4.1 SELECTION OF RAW MATERIAL

2.4.1.1 The Matrix

As already mentioned in 2.1.2.1, to optimize the thermodynamic driving force during sintering, it is necessary to start with a highly reactive powder, with good

morphology and a favourable surface chemistry. These conditions apply just as well to whisker-reinforced ceramic composite. Powder having a sub-micron particle size, and a wide particle size distribution is preferred (in the case of non-oxide ceramics, the quantity of oxygen due to the passive oxide layer on the particle may increase to an undesirable level if the particle size becomes too small; this would be detrimental to the material, due to the formation of weaker phases, such as amorphous silicates). This gives good packing characteristics and thus high green densities, resulting in fast sintering and low shrinkage, and a small average grain size⁽⁶⁴⁾.

2.4.1.2 The Whiskers

It is fortunate that the manufacturers of whiskers go into great effort to optimize the quality of their product. For the production of good whisker-reinforced composites, it is necessary to use whiskers having high purity, with little contaminants (as these may effect the formation of undesired phases), a uniform diameter/aspect ratio, a uniform crystal structure and a compatible surface chemistry. The inclusion of particulates is undesirable⁽⁶⁵⁾.

2.4.1.3 The Liquid Phase

The composition and quantity of liquid phase desired during sintering is also another area where extensive research has been carried out^(64,66,67). In whisker-reinforced composites, the liquid phase has an even more important role than in monolithic ceramics. Due to the rod-like nature of whiskers, good packing is difficult

to obtain, as explained by Mllewski⁽⁶⁸⁾. Therefore the liquid serves primarily as a lubricant to help rearrange particles during the sintering process (according to Kingery's model⁽³⁶⁾). This is when the largest shrinkage rate occurs in the material, and as will be explained later, if this is high enough then full densities will be attained. The liquid phase as a reactant (as opposed to a lubricant) in the sintering process has no ulterior role other than that of sintering (as in monolithic material), unless there is a chemical reaction between this liquid phase and the reinforcing phase. For example, the ever present silica layer on SiC whiskers will dissolve in the liquid phase used to sinter Si_3N_4 , and hence may degrade the whisker properties⁽⁶⁹⁾.

2.4.2 PROCESSING TECHNOLOGY

The philosophy of secondary phase dispersion to reinforce a matrix yields optimum results if there is homogeneous dispersion of the reinforcing phase. Therefore in whisker-reinforced ceramic-matrix-composites (CMC), obtaining a uniform dispersion of the whiskers is essential. This has been the focus of many studies⁽⁷⁰⁾, some of which will be discussed later.

One of the biggest problems in advanced structural ceramics, in general, is the presence of processing flaws in the matrix. The occurrence of these flaws is one of the main causes of early failure. In whisker-reinforced CMC's the problem is further aggravated as processing of whiskers can be a difficult task due to their different surface chemistry and geometry.

One of the major causes of processing flaws is the presence of powder agglomerates, which form as a result of the high affinity of the powder particles to adhere to one another due to their sub-micron diameters, and hence high surface energies. Upon sintering, these agglomerates form regions of low density in a dense matrix. So by eliminating them from the starting powder, and obtaining more homogeneous powder packing, the material properties have been shown to improve⁽⁷¹⁾.

This section deals with the various steps involved in the fabrication of ceramic composites and consists of a brief description of the scientific principles as well as a review of the work done on the subject.

2.4.2.1 Mixing and Dispersion

In a ceramic composite system it is important to have a uniform starting powder, with a homogenous distribution of sintering additives and secondary phase, as well as an agglomerate free matrix material. Because advanced ceramic materials require starting powders of such small particle size, inter-particle attraction prohibits dry mixing of the different powders. Suspension processing is therefore used. A colloidal slip is formed by adding powder to a liquid, such as alcohol or water. To counteract the ever-present attractive forces between the particles, the slip is made *stable* by inducing repulsive forces. The various forces used to disperse suspension are: Brownian Motion, Hydrodynamic forces, Electrostatic forces, Steric forces and Ultrasonic vibrations. A brief description of each follows.

Brownian Motion

This is the result of particles being continually bombarded by other molecules in the medium. This causes the particles to "jump", hence placing them in perpetual motion⁽⁷²⁾. Associated with Brownian motion is diffusion. When a concentration gradient exists in a suspension, there is a gradual migration of particles toward the region of lower concentration by Brownian motion. This is because the number of jumps increases with concentration. Brownian motion is also responsible for the separation of particles, according to size, in a settling column. As particles fall by the action of gravity, a higher concentration is created in the lower portion of the suspension. An equilibrium is reached when the diffusion is balanced by the gravitational acceleration of the falling particle.

Mechanical forces

These are forces induced by mechanical action on the suspension, to help form a more stable slip. Such forces include impact and/or shearing action of media to break up agglomerates of particles, and hydrodynamic forces resulting from mechanically induced shearing occurring between planes of liquid moving at different speeds. Particles moving in different planes are therefore made to collide, or separate, depending on the nature of the force. In ceramic particle systems, these forces have a special significance, since most slips are mixed using a milling techniques, as will be described shortly.

Electrostatic forces

These forces are created as a result of the surface charge on a particle. This then adsorbs counterions onto the surface to become electrostatically neutral. These ions forms a so-called *Diffuse* or *Electric Double Layer* (Fig. 2.9)⁽⁷³⁾. The composition of this double layer is rather complicated, with the formation of a more rigid *Stern layer* and the outer, more mobile *Diffuse layer*. As two particles approach one another, their double layers overlap, and a repulsive force results due to the equal charges. This force is counteracted by the attractive Van der Waals forces, the balance of which is described by the Derjaguin, Landau, Verwey and Overbeek (DLVO) theory⁽⁷⁴⁾. The action of electrostatically shearing the mobile diffuse layer from the Stern layer is an electrophoresis measurement, which in turn give the ζ -potential of a particle. This measurement is also dependent on the ionic concentration of the suspension.

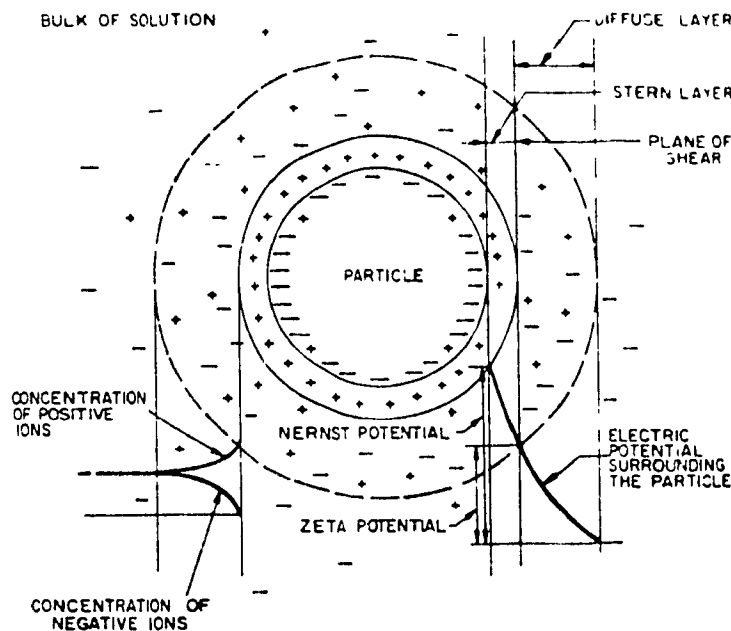


Fig. 2.9: The electrostatic double layer.

Steric forces

These forces are created by the addition of polymeric molecules, which are adsorbed onto the surface of a particle. Essentially, this is a modification of the surface properties of the particle, both physically and chemically. The result is somewhat similar to the electrostatic double layer, where *steric repulsion* results from the interaction of the molecules on the surface (Fig. 2.10)⁽⁷³⁾. The physical basis of the steric repulsion between particles arises from two effects: 1) a volume restriction effect arising from the decrease in possible configurations in the region between the two surfaces of the particles, and 2) an osmotic effect due to the relatively high concentration of adsorbed molecules or chains in the region between the particles as they approach.

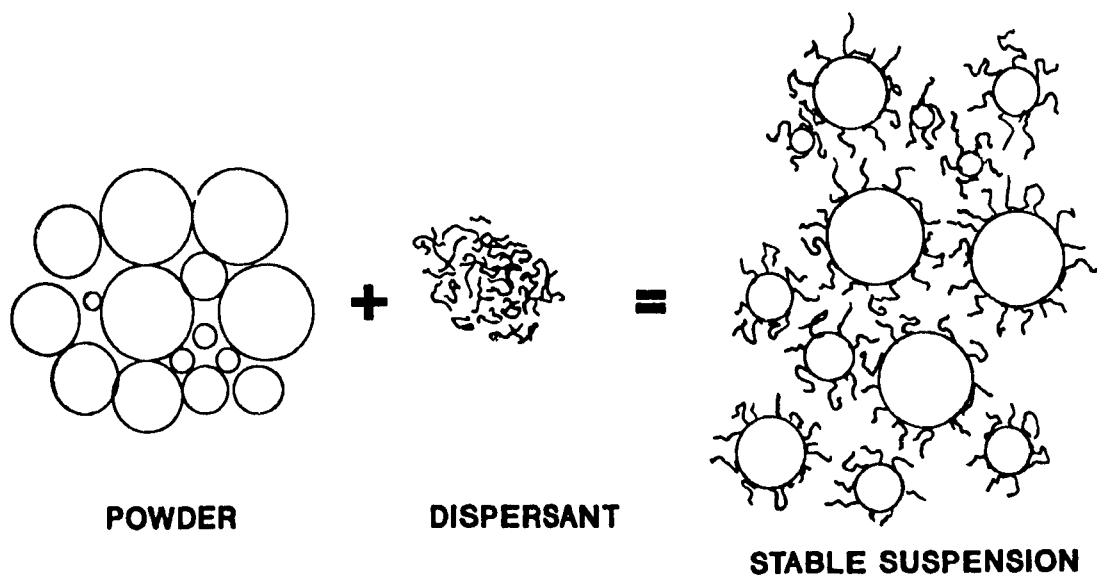


Fig. 2.10: Steric repulsion.

Ultrasonic vibration

Ultrasonic waves may be used to agitate coagulated particles and break them down, thus forming a more dispersed slip. Agglomerates break up as each individual particle attempts to oscillate at the frequency of the waves. However, prolonged agitation should be avoided as there is a tendency for particles to reaggregate. Ultrasonic dispersion is generally used in conjunction with the other methods described above.

Deagglomeration in Whisker Composite Systems

The various deflocculation techniques have all been studied in order to obtain a good dispersion of whiskers in the matrix powder. Milling is still the most commonly used mixing method, be it ball^(64,96,75,76) or attrition milling⁽⁷⁷⁾, although the latter has been shown to be more efficient in obtaining a dispersed slip⁽⁷⁸⁾. In addition, a patented design called turbo-milling was reported to be even more effective⁽⁷⁹⁾ than either ball or attrition milling.

Dispersing the slurry by altering the pH of the slip has also been used successfully. By measuring the pH at which the surface charge of the particles changes from negative to positive, designated the iso-electric point (*iep*), using electrophoresis, it is possible to select a suitable pH to disperse the slip; the farther away the pH of the slip is from the *iep*, the slower the coagulation. For example, Al_2O_3 has been shown to have an *iep* at a pH of ~ 8.0 , and both SiC and Si_3N_4 have an *iep* in the pH range of 6.5-7.0. This is due to the presence of a surface silica layer on both materials, and is

presumed to be the overriding factor^(80,81,82) in determining the surface properties of these non-oxide ceramics. Thus for an $\text{Al}_2\text{O}_3/\text{SiC}_w$ systems a pH of 4.0-5.0^(67,83) or >10.0 ⁽⁸⁴⁾ was used to disperse the slip. A pH of 9.0 has been used to disperse $\text{Si}_3\text{N}_4/\text{SiC}_w$ systems⁽⁸⁵⁾.

The other technique, which has gained popularity in recent years is the use of polymeric dispersants. This method has, to date, been mostly applied to the $\text{Si}_3\text{N}_4/\text{SiC}_w$ system. The dispersants are of the likes of a polyacrylate⁽⁸⁵⁾ or a combination of a polycarbonate and an amine⁽⁷⁰⁾.

2.4.2.2 Consolidation of Whisker-Reinforced Composites

The two most popular fabrication methods to produce test samples are *Pressing* and *Slip Casting*. The main difference between the two is that for pressing, the slurry has to be dried and granulated, whereas in slip casting it is processed as a concentrated suspension. This stage of fabrication reflects the quality of dispersion attained by using the techniques discussed above and can be determined by measuring the density of the green body.

Slip casting of whisker composites always seems to yield higher green densities. For the $\text{Al}_2\text{O}_3/\text{SiC}_w$ system, typically processed by a pH modified slurry, densities of 65-70% of theoretical have been reported for samples containing up to 30 vol% whisker content⁽⁶⁷⁾, when compared to pressed bars giving densities of 50-55%⁽⁶⁴⁾. For the $\text{Si}_3\text{N}_4/\text{SiC}_w$, a similar green density was obtained for the slip cast samples containing up to 20 vol% whiskers⁽⁸⁵⁾. However, cold isostatically pressed samples have been

reported to have green densities of 58-64%^(69,77). For Si_3N_4 this value depends very much on the particular powder characteristics.

Filtration has been used to obtain powder/whisker cake by fast removal of the liquid through the application of external pressure, and gives a similar result to slip casting. Green densities of 59-65% for an $\text{Al}_2\text{O}_3/\text{SiC}_w$ have been reported using this method⁽⁸⁶⁾. Other fabrication methods used to produce green bodies of whisker composites include injection molding⁽⁸⁷⁾. Extrusion, although used widely to form monolithic ceramic components, has never been investigated as a fabrication process for whisker-reinforced CMC's.

2.4.2.3 Sintering

Most of the successful results obtained to date are for composites sintered by either HIPping, with^(77,87,88) or without sintering additives⁽⁷⁰⁾, or using hot-pressing^(66,75,84,86,90). High sintered densities have been obtained without any serious difficulties, except in some cases where a high whisker loading was used. But even here 95% densities have been reported for 20% volume of whiskers⁽⁷⁷⁾. A longer sintering time has been used to obtain high densities for 30% whisker content⁽⁹⁰⁾. The use of hot pressing methods, although unsuitable for most commercial applications, has enabled researchers to analyse the various mechanisms in the material, such as densification kinetics, and study the ways in which the material responds to varying parameters such as whisker content and sintering additives.

Although dense composites may be produced by hot-pressing techniques, it is

limited primarily by the expenses involved in equipment and operation. Furthermore, only simple shapes may be produced using hot-pressing, and whiskers tend to orient themselves perpendicular to the direction of pressing as a result of the uniaxial pressure applied to the samples during sintering⁽⁹²⁾.

The drive to produce whisker composites using a cheaper, more practical method, such as pressureless or gas pressure sintering, is evident. Pressureless sintering usually requires samples with high green density to minimize shrinkage. Whiskers do not allow for large shrinkages, since whisker bridging causes problems. When bridging reaches a critical point, a skeletal network forms in the matrix, inhibiting further densification^(64,83). Fig. 2.11 shows the way in which sintered density decreases with increasing whisker content. This problem could be minimized by increasing the amount of liquid phase^(64,77), or by reducing the aspect ratio of the whiskers^(68,88). Indeed sintered densities >95% has thus been produced for composites with up to 20% whisker

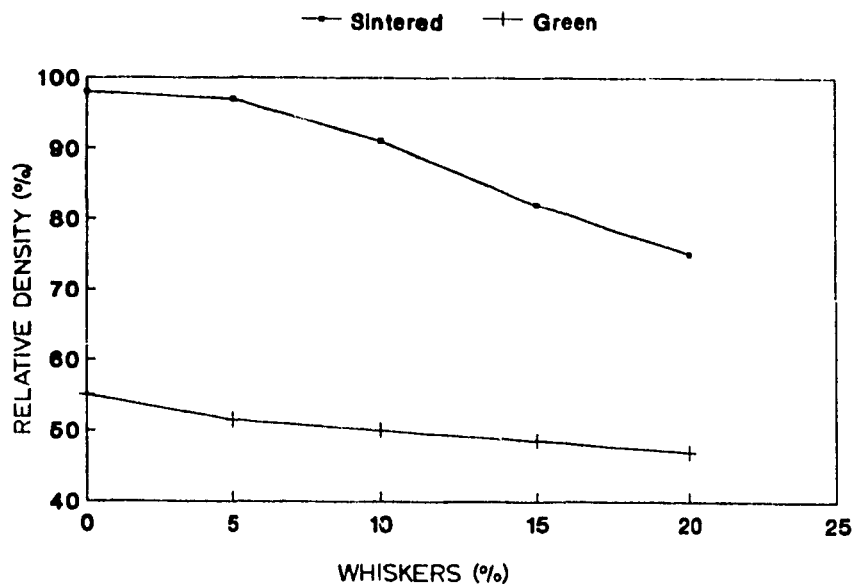


Fig. 2.11: The effect of whisker content on density for pressureless sintered specimens⁽⁹³⁾.

content⁽⁷⁷⁾. However in both cases, there is a sacrificial reduction in strength. The use of gas pressure sintering has been reported to produced dense samples of up to 20% whisker content, at pressures of 10MPa⁽⁷⁷⁾. But even in this case, as much as 35% sintering additives had to be used to achieve this. Pressureless sintering of slip cast specimens shows promising results. Because of the high green densities produced by slip casting, it looked like a promising fabrication method. Table 2.2 shows the densities obtained for a $\text{Si}_3\text{N}_4/\text{SiC}_w$ system produced using slip casting⁽⁸⁵⁾. The only

Table 2.2: Densities for slip cast and CIP specimens.

WHISKER CONTENT (VOL.%)	SLIP CASTING		C.I.P.	
	GREEN DENSITY (% R.D.)	SINTERED DENSITY (% R.D.)	GREEN DENSITY (% R.D.)	SINTERED DENSITY (% R.D.)
0	69.1	98.5	64.0	99.5
5	68.3	98.5	63.8	99.5
10	67.8	96.9	61.0	97.0
15	65.9	94.5	60.5	94.5
20	64.0	88.5	55.7	88.5

disadvantage of this method is the anisotropic shrinkage behavior resulting from whisker alignment along the surface of the mold. Similar detailed work in this area was carried out on $\text{Al}_2\text{O}_3/\text{SiC}_w$ which yielded densities of 97% and 92% for whisker loadings of 15% and 27%, respectively⁽⁶⁷⁾.

Another sintering method used exclusively for the $\text{Si}_3\text{N}_4/\text{SiC}_w$ system is by reaction bonding. A Si/SiC_w compact is nitrided to grow Si_3N_4 from the silicon powder⁽⁹⁴⁾. This process is generally followed by a hot-pressing⁽⁹⁵⁾ or HIPping⁽⁶⁹⁾ step

to densify the body to full density, and obtain improved properties. Fig. 2.12 shows the increase in density after each step of sintering, for whisker content up to 30%.

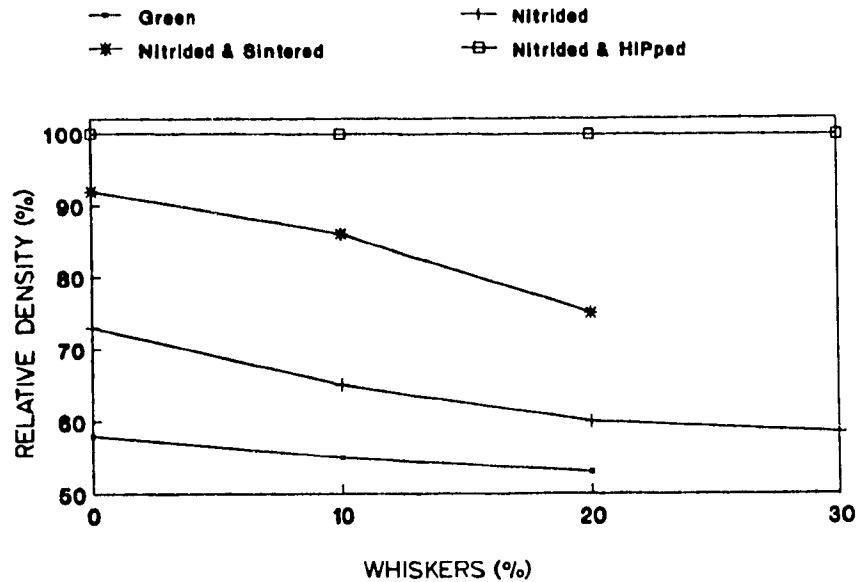


Fig. 2.12: Density increase using various sintering methods⁽⁶⁹⁾.

2.4.3 MECHANICAL PROPERTIES

Whisker reinforcement has been shown to improve the mechanical properties of a ceramic material. Table 2.3 shows the strength and toughness values for a hot-pressed $\text{Al}_2\text{O}_3/\text{SiC}_w$ composite, for whisker loading of up to 40%⁽⁹⁶⁾. Generally, properties improve with increasing whisker content, but at high whisker loading, problems of low density seem to effect mechanical properties.

Table 2.4 shows a summary of the properties obtained for the $\text{Si}_3\text{N}_4/\text{SiC}_w$ system by various researchers⁽⁹¹⁾. Although an increase in toughness is almost always

Table 2.3: Mechanical properties of Hot-Pressed Al₂O₃/SiC_w composites⁽⁹⁶⁾.

WHISKER (VOL.%)	TEMP. (°C)	K _{1c1/2} (MPa.m ^{1/2})	M.O.R. (MPa)
0	22	4.5	-
	700	4.0	-
	1000	3.8	-
10	22	7.1	455
	1000	-	320
20	22	7.5-9.0	655
	700	-	535
	1000	7.0-8.0	570
40	22	6.0	850
	700	-	740
	1000	6.2	665

evident, the way in which the strength values behave is not clear yet, as the results differ somewhat. As mentioned earlier, the properties of Si₃N₄ starting powders vary from one producer to another, and this could be one of the causes of disagreement. However, it is certainly clear that the inclusion of whiskers in a ceramic matrix hinders the propagation of the crack. It has also been shown that the orientation of these whiskers can have a significant effect on the toughness of the material, reaching a maximum when the whiskers lie in a plane perpendicular to the path of the crack⁽⁹²⁾.

The toughening mechanisms identified to be acting include crack deflection or branching, resulting from stresses created due to thermal expansion coefficient mismatch, and whisker bridging behind the crack, with pull-out contributing to some extent^(58,76,84).

Interfacial bonding has once again been attributed to having a large effect on the toughening of the composite material, mostly due to the fact that whisker

Table 2.4: Mechanical properties of various $\text{Si}_3\text{N}_4/\text{SiC}_w$ composites⁽⁹¹⁾.

WHISKERS (VOL.%)	M.O.R. (MPa)	$K_{Ic}^{1/2}$ ($\text{MPa}\cdot\text{m}^{1/2}$)	TEMP. ($^{\circ}\text{C}$)
0	375	4.0	25
	900	6.0	25
	780	4.7	25
	575	4.9	1000
	480	6.2	1200
	660	7.1	25
10	625	5.5	25
20	550	7.0	25
	575	5.0	25
30	970	6.4	25
	820	7.5	1000
	590	7.7	1200
	450	10.5	25

bridging/pull-out requires that the crack propagates along the interface. Indeed, a strong interfacial bond has been shown to decrease the toughness of the whisker-reinforced material^(66,69). It has been proposed that by modifying this interface, higher toughness values may be obtained⁽⁵⁸⁾. However attempts thus far have not yielded any major improvement in strength and toughness^(91,97).

2.4.4 HIGH TEMPERATURE PROPERTIES

Due to the potential high temperature applications of whisker-reinforced ceramics, it became necessary to know the behavior of these material. There are a number of factors that have to be considered when performing and analysing experiments at high temperatures: there is a strong dependence on temperature and

time; the liquid phase, if present plays a very important role, creep becomes a controlling factor, failure modes change and cracks becoming more stable as the material becomes more ductile in nature.

In Table 2.3, high temperature strength values are also presented for varying whisker content. Strength retention, even at elevated temperatures, is evident, although this has been shown to decrease as temperature increases⁽⁸⁹⁾. Creep is believed to cause this strength degradation. Toughness on the other hand was seen to increase, due mostly to the softening of the grain boundary bonding phase.

It has been reported that creep rates for a 5% SiC whisker reinforced alumina material are significantly lower (of the order of two) than that of a monolithic material, at temperatures of up to 1500°C⁽⁹⁸⁾. Furthermore, as whisker loading increases, the creep rate decreases, and the material does not follow a steady-state relationship. The proposed mechanism suggests that the whiskers provide a mechanical restraint to grain boundary sliding.

2.5 SUMMARY

From the above literature review, it becomes apparent that there is a demand for ceramic materials with improved toughness characteristics, and whisker reinforcement appears to be a strong contender in this field. A process involving the more economic and versatile densification method of pressureless sintering would be most desirable,

and as mentioned above, the ability to preferentially align whiskers within the material should lead to enhanced toughening. In addition, the use of a green fabrication process giving such alignment would decrease the problem connected with whisker bridging and skeletal network formation during sintering.

From these observations, the objectives of this work were outlined and are listed in the following chapter.

3. OBJECTIVES

The aim of this work is:

- 1) To study the dispersion behavior of UBE Si_3N_4 whiskers and UBE Si_3N_4 powder using two different methods.
- 2) To obtain a reinforced Si_3N_4 matrix by the introduction of acicular single crystals of Si_3N_4 , in the form of whiskers, such that a matrix with elongated grains results, and to develop a processing method to produce a dense, reinforced material.
- 3) To obtain this densification of the matrix by pressureless sintering, using only the aid of a liquid phase and to study the densification mechanism of such a composite material.
- 4) To investigate the use of Hydroxypropyl Cellulose as a plasticizer during processing.

4. EXPERIMENTAL PROCEDURE

4.1 RAW MATERIAL CHARACTERIZATION

The Si_3N_4 powder used in this work was a fine grained, high purity powder, previously determined to have good sintering characteristics⁽⁹⁹⁾. The specifications of the powder (SN-E-10)* are shown in Table 4.1, as are those for the Si_3N_4 whiskers (SN-E- β w), also from the same source. Figs. 4.1 is a secondary electron micrograph of the whiskers, showing aspect ratios ranging from 15-50, and an average diameter of approx. $1\mu\text{m}$.

Table 4.1: Specification of starting powder and whiskers.

GRADE		POWDER SN-E-10	WHISKERS SN-E- β w
MORPHOLOGY		EQUIAXED	ACICULAR
PARTICLE SIZE		$d = 0.1-0.3\mu\text{m}$	$L/d = 15-50$
SPEC. SURF. AREA		$10-14\text{m}^2/\text{g}$	$2.43\text{m}^2/\text{g}$
PURITY	N	>38.0%	40.0%
	O	<2.0%	0.45%
	C	<0.2%	
	Cl	<100pp	
	Fe	<100ppm	<800ppm
	Ca	<50ppm	<50ppm
	Al	<50ppm	<50ppm
	Y		0.5%
PHASE COMPOSITION		100% Crystalline α PHASE=95% β PHASE=5%	100% Crystalline β PHASE=100%

*UBE Industires Ltd.

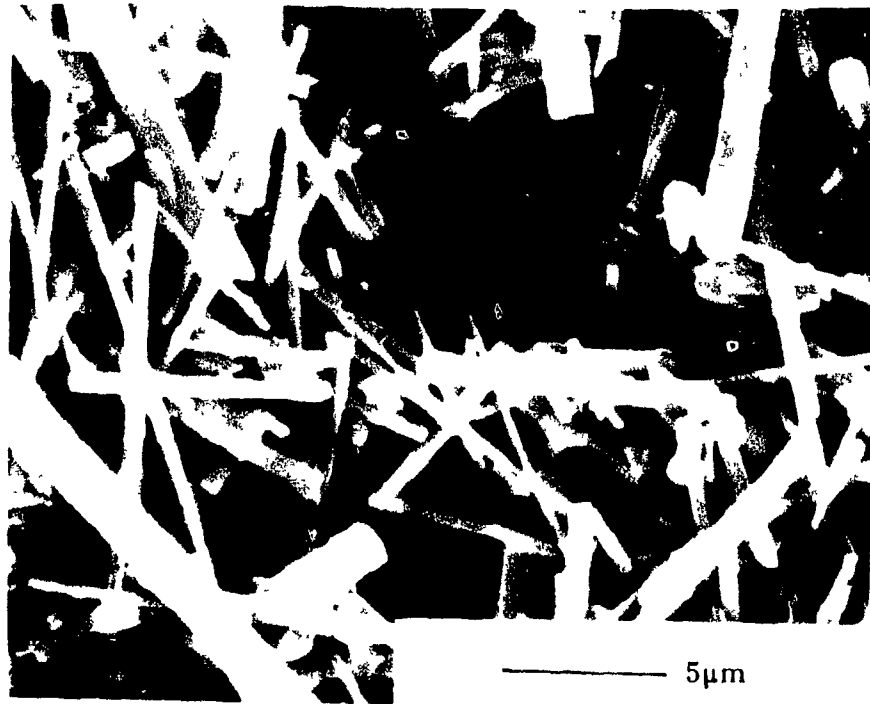


Fig. 4.1: UBE Si₃N₄ whiskers.

Sintering additives used to aid the densification process were Aluminium Oxide (Al₂O₃)^{**}, Aluminium Nitride (AlN)^{***}, and Yttrium Oxide (Y₂O₃)^{****}. The composition of the mixture is shown in Table 4.2. The total additive content was 11.25% by weight. The theoretical sintered density for this powder was calculated to be 3.27 g/cm³. As the powder and whiskers are of the same material (Si₃N₄), they both have the same density (3.18 g/cm³), and thus whisker additions in weight % and volume % are equivalent.

^{**}A16SG Alcoa

^{***}Grade C, H.C. Starck

^{****}5603, Molycorp

Table 4.2: Composition of starting powder mixture.

POWDER	WEIGHT%
$\text{Si}_3\text{N}_4+\beta\text{w}$	88.74
Al_2O_3	4.97
AIN	1.72
Y_2O_3	4.56

4.2 POWDER DISPERSION AND MIXING

The Si_3N_4 powder, including the additives and the whiskers, were mixed in the wet state. Varying weight fractions of the whiskers were mixed with the powders. These were added to a liquid, generally water or iso-propyl alcohol and dispersed as a colloidal suspension, using one of the following methods: attrition milling and ultrasonic dispersion, or pH adjustment. These methods are outlined below.

4.2.1 ATTRITION MILLING/ULTRASONIC DISPERSION

Fig. 4.2 is a flow diagram of this dispersion method. The powder/whisker mix was attrition milled in iso-propyl alcohol, or water at a speed of 200rpm for 30 minutes. The ratio of liquid to powder was 5 parts to 1, by weight. Silicon nitride milling media having a diameter of $\approx 5\text{mm}$ was used, in the proportion of 3 times the weight of the powder used. After mixing, the slip was poured through a $212\mu\text{m}$ sieve

into a beaker. It was then sonicated for 30 minutes using an ultrasonic bath and an ultrasonic probe at 115 Watts. The slip was milled again for another 20-30 minutes using the same conditions as above. The liquid was removed by drying in a microwave oven, as will be explained in section 4.3 below.

4.2.2 pH ADJUSTMENT

The procedure used for this dispersion method is outlined in Fig. 4.3⁽⁸⁴⁾. The powder/whiskers were added to de-ionized water to a solids loading of 15% by weight. The pH of the suspension was then adjusted to >10.0 by adding NH_4OH while stirring.

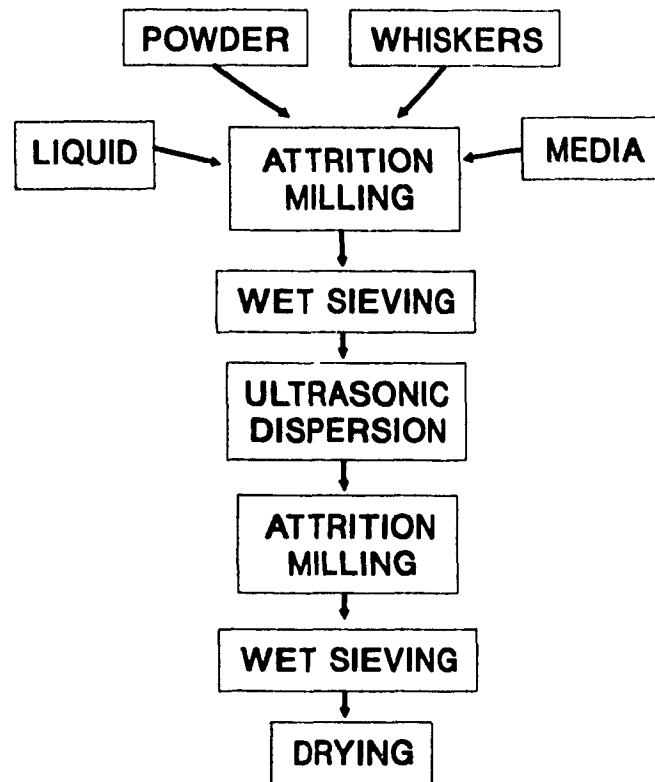


Fig. 4.2: Processing route for attrition milling whiskers and powder.

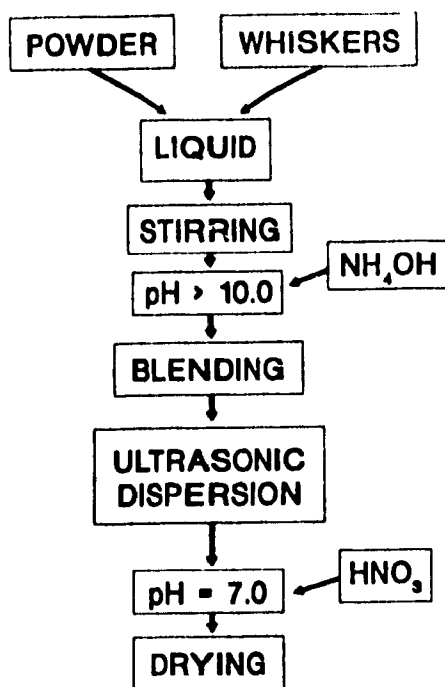


Fig. 4.3: Processing of whiskers and powder using pH adjustment⁽⁸⁴⁾.

The slip was agitated using a high speed blender for 5 minutes. After being transferred into a beaker, it was further dispersed in an ultrasonic bath for 5-10 minutes, using both the bath and the probe as described in 4.2.1 above. The pH of the suspension was then adjusted to 7.0 by the addition of nitric acid. The slip was later dried as discussed in 4.3, below.

4.3 DRYING AND GRANULATING

Drying was carried out using two different methods: microwave drying, and by

boiling off the excess water. In most of the experiments, the microwave drying technique was used. However some suspensions prepared by the pH adjustment method (section 4.2.2), were dried by boiling off the excess water while stirring, until the solids loading of the slip reached 40%. It was then completely dried in a conventional oven at 130°C.

The resulting large aggregates of dry powder and whiskers were then granulated through a 212 μ m sieve so as to form a free flowing powder which could later be used to fabricate samples.

4.4 FABRICATION OF SAMPLES

Samples for density and mechanical testing were prepared using two different methods, namely pressing and extrusion.

4.4.1 PRESSING

Fig. 4.4 shows a flow diagram for the fabrication of samples by this method. Approximately 2g of the dry granulated powder/whisker mixture was uniaxially die pressed at a pressure of 4.6MPa. The resulting bars had a rectangular cross-section and dimensions of approx. 42x7.5x4mm. The bars were subsequently isostatically pressed at 340MPa, after which they were dried at 130°C for 1 hour.

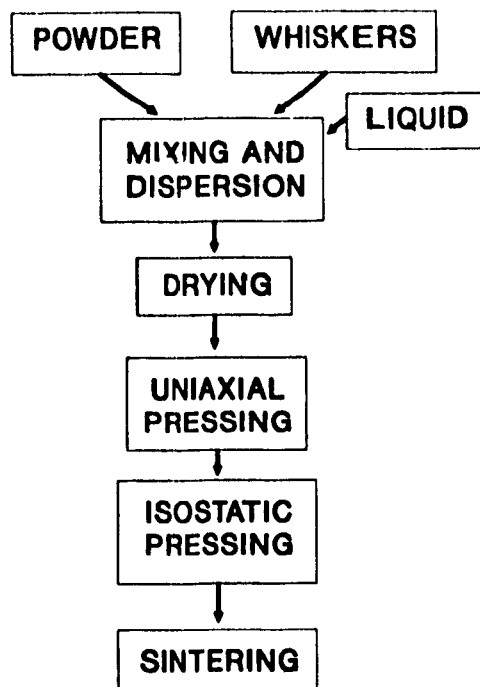


Fig. 4.4: Processing route for fabricating pressed bars.

4.4.2 EXTRUSION

The second fabrication method involved extruding the powder/whisker mixture, after it had been formed into a paste by the addition of a plasticizer (Hydroxypropyl Cellulose (HPC)*, or Methyl Cellulose**). The ratio of powder mixture to plasticizer was optimized at 26:1, by dry weight. The processing route is shown in Fig.4.5. The dispersed, dry, granulated powder was added to the plasticizer which had previously

* 19,189-2, Aldrich Chemicals Co. Ltd.

** 20-213, Methocel, Dow Chemical Co.

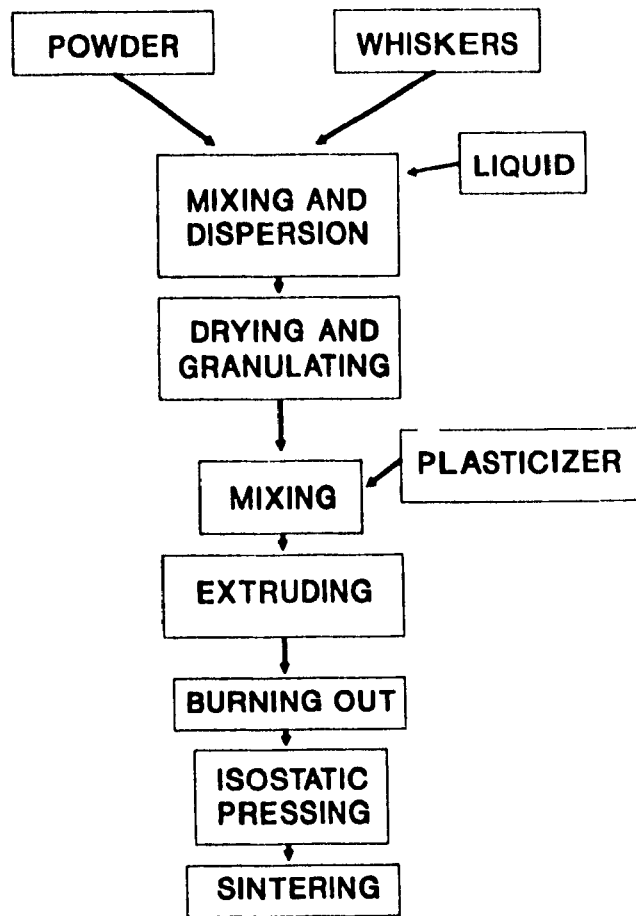


Fig. 4.5: Processing route for fabricating extruded samples.

been dissolved in water. Methyl Cellulose dissolves readily in warm water whereas HPC does not. It needs to be added to water above 40°C and allowed to cool, where it then goes into solution on cooling below 40°C^(100,101). The optimum viscosity of the plasticizer was obtained by mixing 1g of HPC to 7.5ml of water. The paste was continuously stirred during the mixing; in some cases a high speed mixer being used in an effort to improve the paste properties. The paste was then introduced into the barrel of a piston type extruder. Various nozzle designs were used to try and optimize

extrusion conditions, with respect to densification of the samples. The paste was then extruded. Generally, two extrusions were carried out. On occasion, the paste was first extruded through a mesh of 1mm opening, into a vacuum chamber and then collected and re-extruded through the nozzle. The extrudate was dried at room temperature for several hours. The organic plasticizer was then burnt out by heating the extrudate in a furnace for at least 2 hours at 500°C. Samples were made by breaking off lengths of the extrudate (about 30-50mm), which were then isostatically pressed as explained in section 4.4.1 above.

4.5 SINTERING

Once the powder was compacted into shape and dried, the density of the green body was measured. The green density of the samples was calculated by dry weight and dimensions.

The green samples were densified by sintering in a water cooled, controlled atmosphere, graphite element furnace, shown schematically in Fig. 4.6. The sintering temperature ranged from 1750°C to 1800°C, and was maintained for 1 hour. All experiments were carried out in a high purity nitrogen atmosphere at 101-126kPa. The samples were placed in a BN crucible, embedded in a loose BN/Si₃N₄ powder mixture.

The extent of densification was measured by calculating the density of the samples after sintering using Archimedes' principle as laid out in ASTM C373-72⁽¹⁰²⁾.

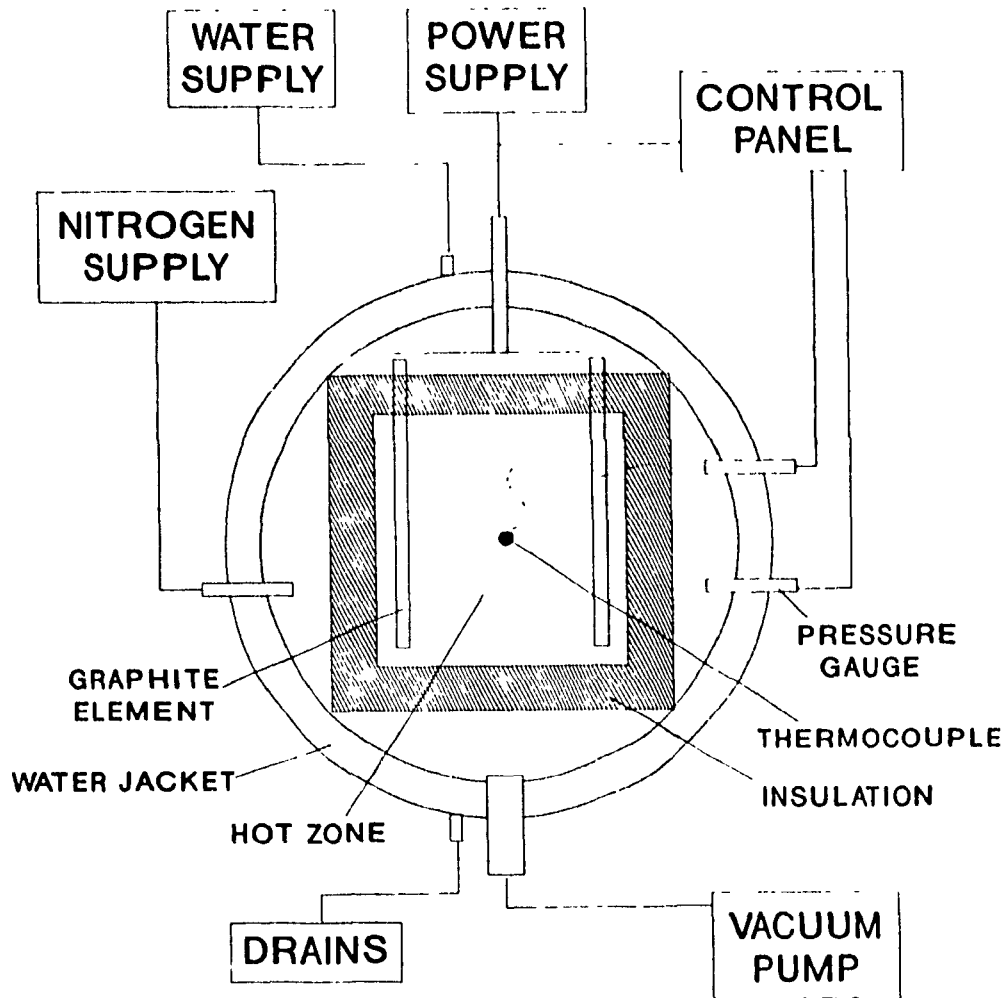


Fig. 4.6: A schematic of the sintering furnace.

4.6 SAMPLE PREPARATION FOR MECHANICAL TESTING

Strength and fracture toughness values were determined using four-point bending (Modulus of Rupture), as shown in Fig. 4.7 and crack indentation measurements (K_{Ic}) respectively⁽¹⁰³⁾.

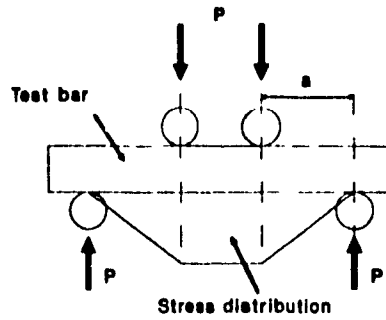


Fig. 4.7: 4-point testing of ceramic samples.

4.6.1 MODULUS OF RUPTURE

Samples were surface ground with a 240 grit diamond wheel to ensure flat, parallel surfaces⁽¹⁰⁴⁾ and the edges were bevelled to remove any stress concentrations.

The M.O.R. was calculated using the equation:

$$M.O.R. = 3Pa/bd^2 \dots\dots\dots(1)$$

where P is the load at fracture, a is half the distance between the point loads (Fig. 4.7), and b, d are respectively the width and thickness of the specimen.

4.6.2 TOUGHNESS

Samples were prepared by first polishing them to a $1\mu\text{m}$ finish, as will be explained in 4.7 below. They were then indented with a diamond indenter*, using a

* Vicker's Indentation

50kg load. The length of the crack, c , and the size of the indent, a , were measured using an optical microscope and K_{Ic} values were calculated using the equation⁽¹⁰³⁾:

$$K_{Ic} = 0.015 ((c-a)/a)^{-1/2} (E/H)^{2/3} (P/c^{3/2}) \dots\dots\dots(2)$$

where E = Young's modulus, H = hardness, and P = load. This equation is a modification of the one developed by Lawn *et al.*⁽¹⁰⁵⁾, and takes into account the Palmqvist shape of cracks, which is more representative in crystalline ceramics.

4.7 PREPARATION FOR MICROSCOPICAL EXAMINATION

Microscopy was carried out using several different techniques including Scanning Electron Microscopy*, reflected and transmitted optical microscopy. The different preparation procedures used for the various samples are outlined below.

Powder samples for SEM analysis were prepared by filtering a highly dilute suspension of powder in a liquid (usually water or iso-propyl alcohol). The suspension was first dispersed by sonicating with the ultrasonic probe for a few minutes. A sample of the suspension was then passed through a filter paper having openings of 0.1-0.4 μ m. After drying, part of the filter paper was placed on an SEM stub and was gold sputter coated prior to observation in the SEM.

Powder samples were also viewed through the transmission optical microscope.

* JEOL T-300

A dilute suspension of powder and HPC plasticizer was mixed in the same manner as in section 4.4.2 above, i.e. manually and using a high-speed mixer. A small amount of plasticizer/powder mixture was placed between two glass plates and lightly pressed. During viewing by transmitted light microscopy they were further pressed and sheared to remove air pockets, and break down any agglomerates.

The green microstructure was analysed by observing fracture surfaces. The green bars were analysed either after burn-out treatment of the polymeric additives, or after isostatic pressing. The samples were fractured in appropriate planes that were of most interest to this work. The pieces were then mounted onto an aluminum stub using an adhesive. All green bars were coated with gold prior to viewing.

Microstructural analysis was also carried out in sintered material in both the fractured and polished state after coating with gold. Planes of particular interest were examined by observing polished surfaces. Samples were first mounted in an epoxy resin mould, or a bakelite mould, followed by coarse diamond grinding, and finally diamond polishing to $1\mu\text{m}$. The samples were then removed from the resin; complete removal being obtained by burning off the epoxy at 500°C . The specimens were etched, using either molten NaOH or KOH for 15 seconds, or hydrofluoric acid for ~30 seconds.

The results obtained by using all the above procedures will be presented and discussed in the next chapter.

5. RESULTS & DISCUSSION

This study compares the fabrication of a Si_3N_4 composite by two techniques: the first being the more conventional pressing method, the other an extrusion method developed specifically for this work.

5.1 PRESSING

5.1.1 POWDER/WHISKER DISPERSION

A study of the dispersion behaviour of the whiskers in the powder was carried out by fabricating samples using uniaxial and isostatic pressing. Different whisker contents were used, ranging from a control sample with no whiskers up to 30% weight content. For each composition, the two different dispersion methods were used (milling and pH adjustment) as described previously. The homogeneity of the dispersion is reflected in the manner in which the powder and whiskers pack to form green bodies. A comparison of the green densities for varying whisker content is shown in Fig. 5.1. Each value is the average of 9-11 samples in the range of $\pm 0.5\%$. The pH method gives slightly higher densities than the milling method. This could be as a result of the presence of NH_4NO_3 which forms from the hydroxide and acid used to regulate the pH of the slip during mixing (4.2.2). In fact, when a sample of 46g of powder/whiskers was

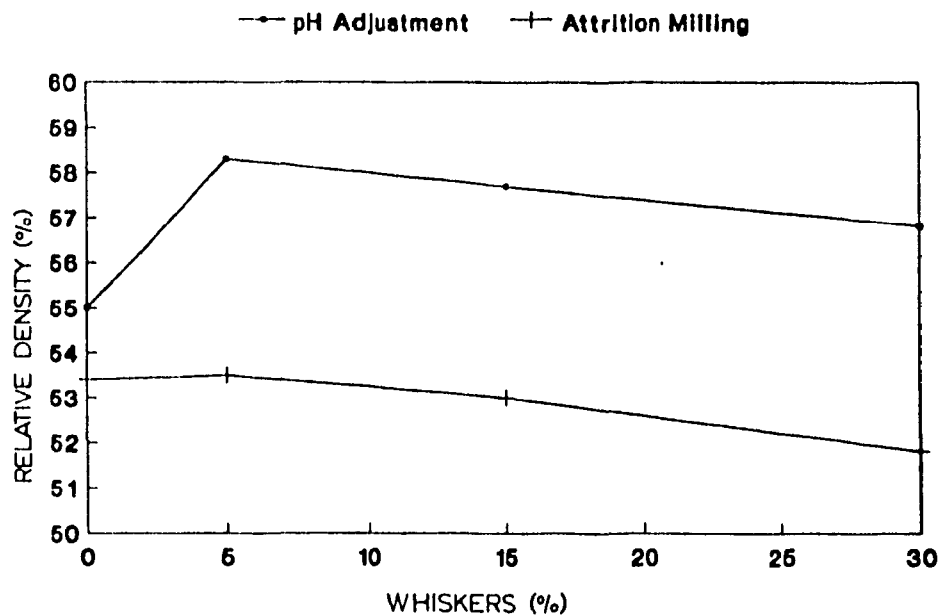


Fig. 5.1: Relative green density vs. whisker content.

burnt out at 500°C to remove the salt, a weight loss of 0.7g (1.5%) was registered. The presence of this salt may have aided packing of the powder by acting as a binder. During the drying stage of processing, the resulting powder cake was much harder to granulate than the cake obtained from the milled powder, possibly due to the bonding effect of the salt. Even after granulation, the 212µm agglomerates would still be partially bonded by the salt. Thus the pressed bar would have an improved overall powder packing, giving the better green density.

The density increased slightly upon addition of 5% whiskers, especially for the bars prepared by pH adjustment, possibly due to the presence of a bimodal particle size distribution, and decreased as the whisker content increased beyond this point.

However the variation in green density is actually very small, ranging over only ~3%.

The improved green density shown by the pH adjusted samples did not result in any improvement in sintered density. In fact the values obtained for both methods were practically identical (Fig. 5.2). As expected, the sintered densities dropped dramatically with increasing whisker content. This behavior has already been reported in previous work, and it is apparent that the presence of whiskers inhibits the densification mechanism⁽⁶⁴⁾; as discussed in section 2.4.2.3.

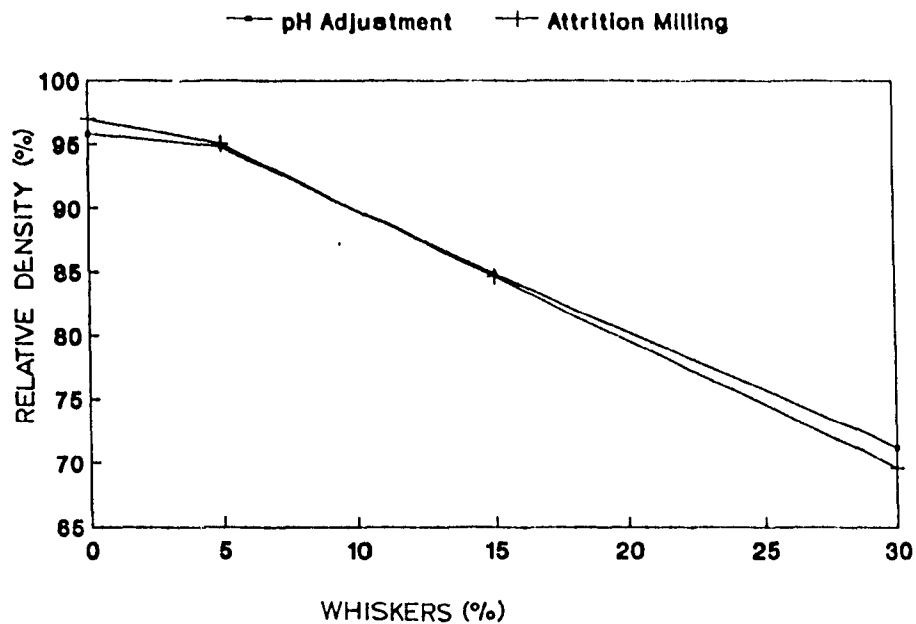


Fig. 5.2: Relative sintered densities vs. whisker content.

5.1.2 MICROSTRUCTURAL ANALYSIS AND DENSIFICATION

An analysis of the microstructure of a fractured green surface (Fig. 5.3) shows good dispersion of the whiskers in the powder for samples prepared using both methods.

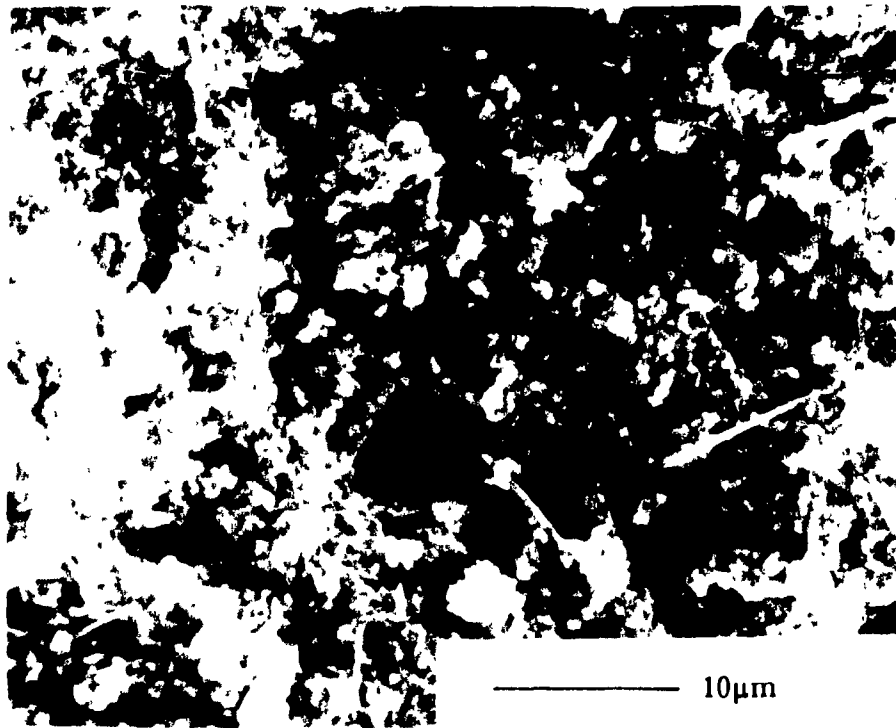


Fig. 5.3: Fractured surface of green compact (15% whiskers).

However it is evident that as the volume content of whiskers increases, more of the whiskers come into contact with one another. As the whiskers themselves do not shrink, this effect is enhanced whilst the body is shrinking during sintering. Since these β -whiskers are thought to be stable through the whole temperature range of sintering (as discussed in 2.1.1), a point is reached where these whiskers form an interlocking network which prohibits any further shrinkage. Thus the liquid phase is unable to promote efficient particle rearrangement and furthermore, the capillary pressure is insufficient to overcome the bridging effect of the whiskers. As a result, porosity is observed in the whisker composite, which increases with whisker content.

Analysis of a fractured surface of a sintered sample containing 30% whiskers

shows an acicular Si_3N_4 microstructure (Fig. 5.4). This contains both the original β -whiskers, and the α powder which has transformed to β crystals, during liquid phase sintering, as described in 2.1.2.2. Fig. 5.5 is an X-ray diffraction scan ($15-45^\circ$) of a pulverized sample and confirms that the material contains no α phase, implying that transformation to β was complete. At high whisker loadings, it is difficult to distinguish between the two forms of β phase. It has been reported that in a monolithic Si_3N_4 , much of the α to β transformation occurs after densification of the bulk material⁽⁴⁷⁾. If this is also the case in the whisker composite material, as is believed, then, due to the whisker bridging process and resulting porosity, the α - β transformation can take place by a vapour-liquid-solid growth mechanism into these pores, as shown schematically in Fig. 5.6(a). If the whisker content is high enough, the transformed

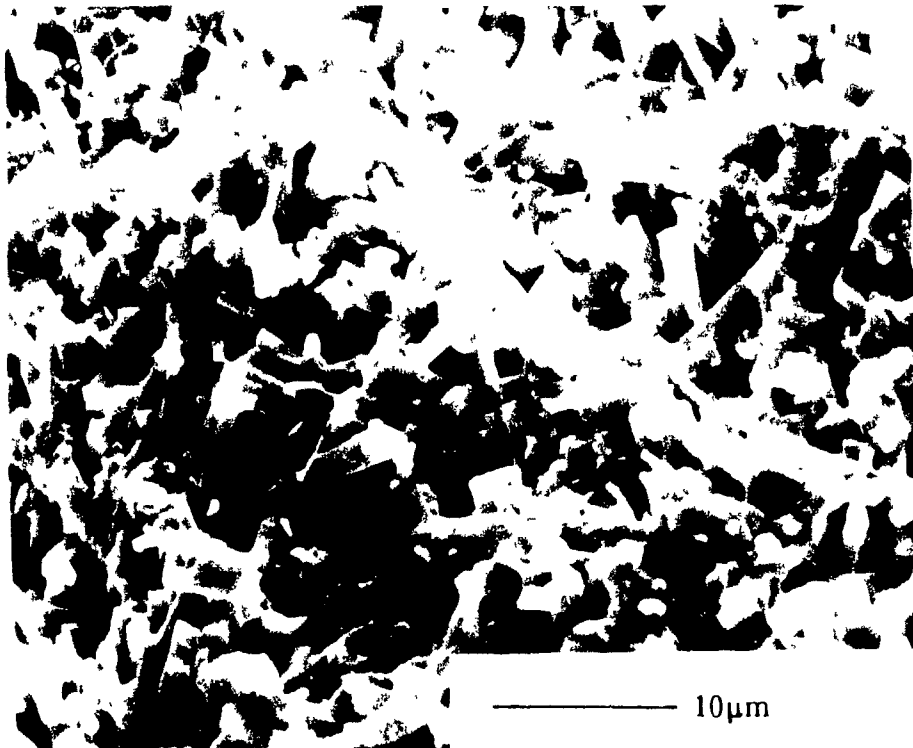


Fig. 5.4: Fractured surface of Si_3N_4 with 30% whisker content.

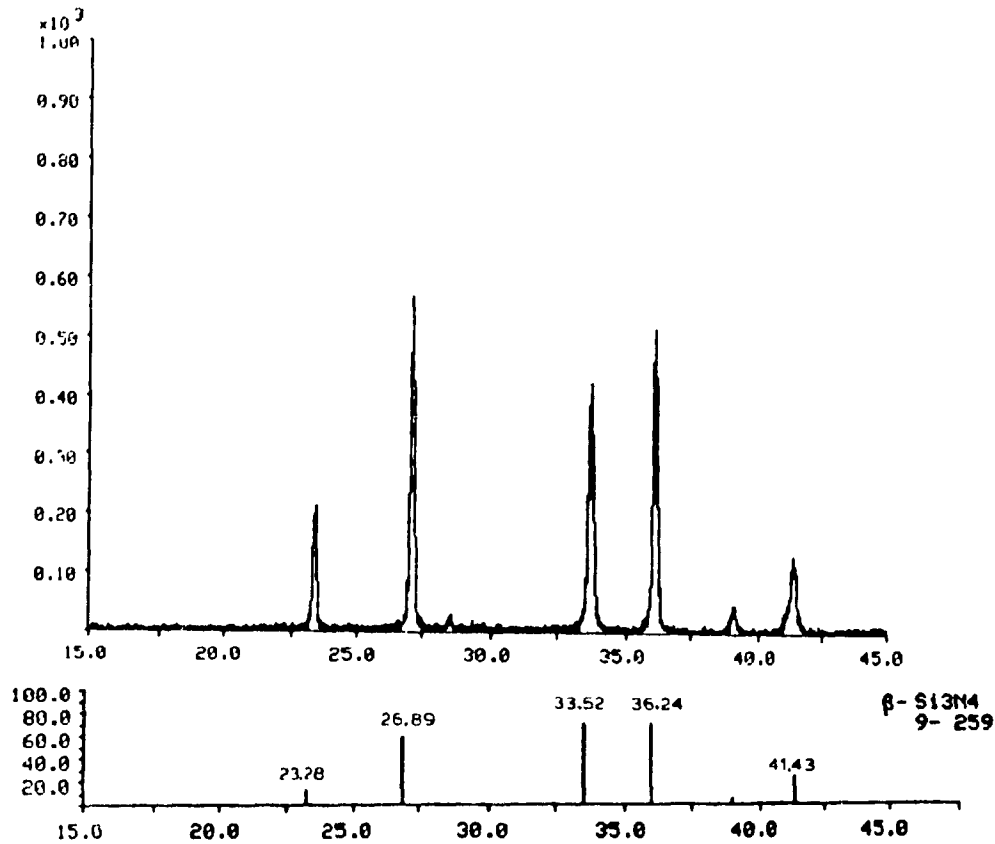


Fig. 5.5: X-ray diffraction of sintered β - Si_3N_4 (30% whiskers), compared to a standard.

grains have enough space to grow to a size comparable to the original whiskers, thus making it difficult to distinguish between them (Fig. 5.7).

During the sintering of this material, it is also possible for powder to get entrapped inside the whisker network. This powder would then shrink more than the bulk material around it due to the jamming effect, and as a result, the material would shrink away from the bulk material, thus forming more porosity, as shown in Fig. 5.8 and schemetically in Fig. 5.6(b).

It is therefore apparent that the sintering mechanism of this material is characterised by the two proposed mechanisms shown in Fig. 5.6. Both mechanisms

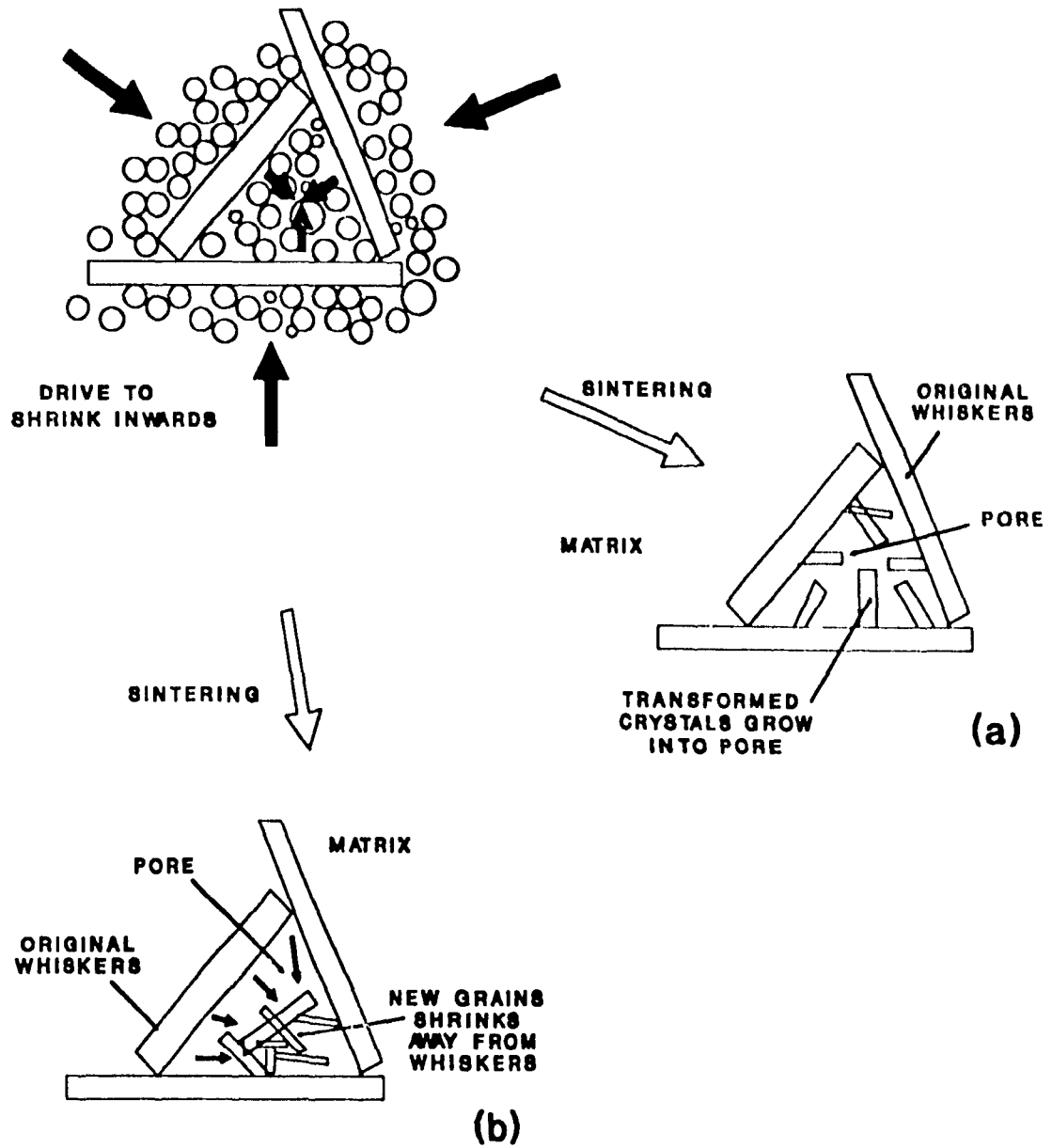


Fig. 5.6: Schematic of the whisker bridging effect which jams densification, a) vapour-liquid-solid growth, and b) shrinking of entrapped powder.

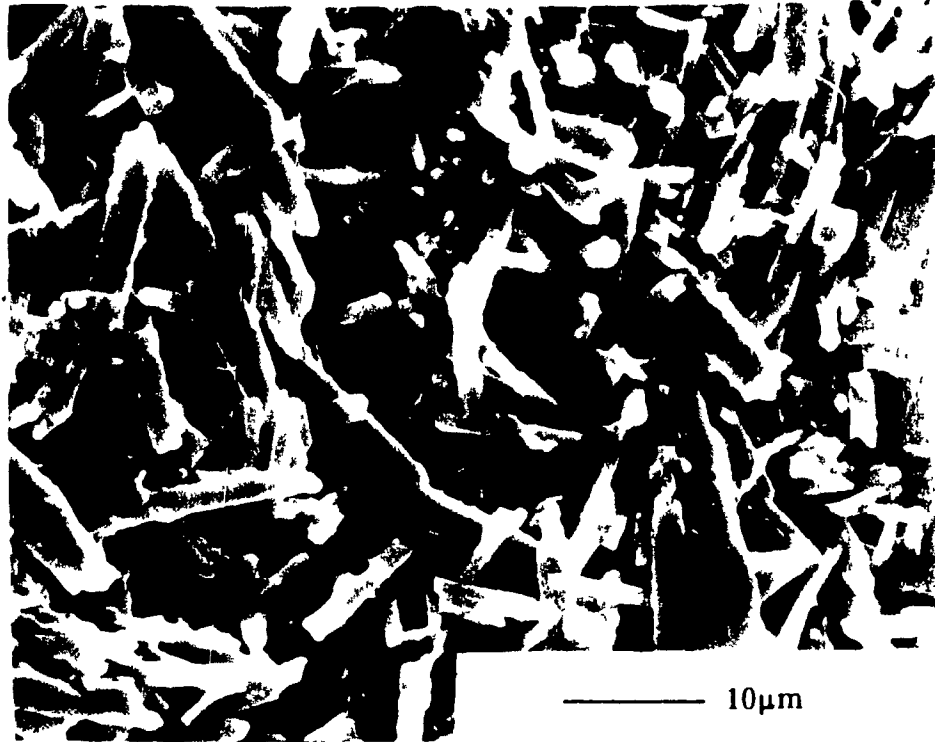


Fig. 5.7: Polished surface of Si₃N₄ with 30% whiskers (NaOH etch).

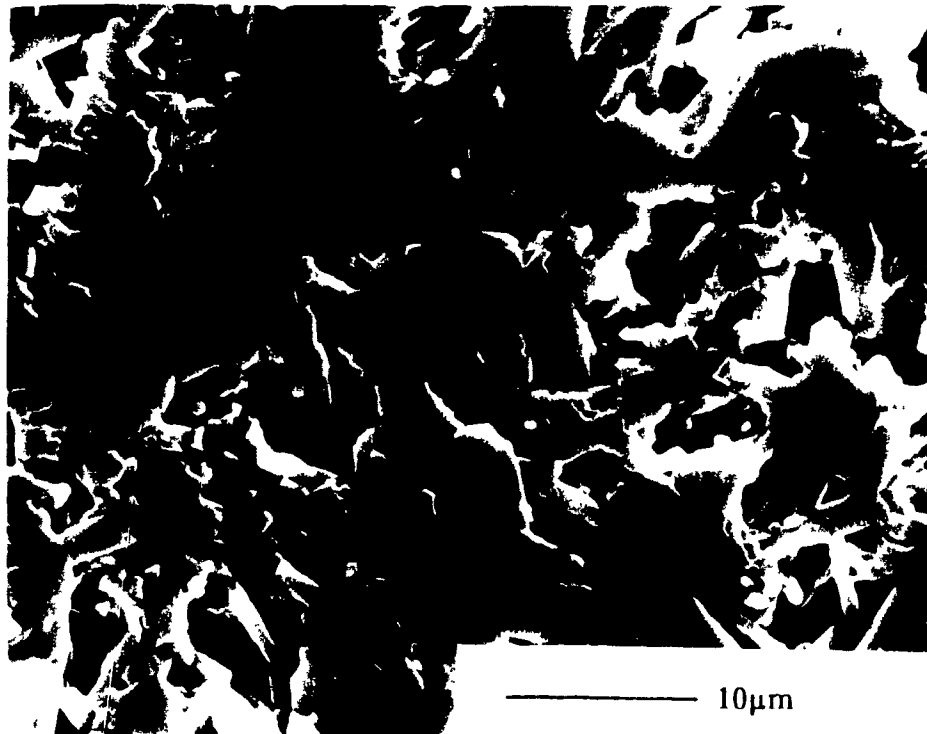


Fig. 5.8: Polished surface of Si₃N₄ with 15% whisker content.

occur simultaneously such that around a bridge of whiskers, there is growth of crystals into the space between the whiskers, which may be occupied by material which shrinks away from the whiskers.

In a polished microstructure of a sample having only 5% whisker content, large grains were clearly present (Fig. 5.9). It would be unlikely for any new β grain to grow to such a large length and aspect ratio when transforming from the α -phase, and it is therefore safe to assume that these large crystals are the original β whiskers. Apparently these whiskers do not seem to have decomposed in any way during the sintering process, and close examination of the micrograph further reinforces the argument of the formation of the skeletal network. Moreover, it appears that the size and aspect ratio of these larger crystals seemed to have changed (this point will be

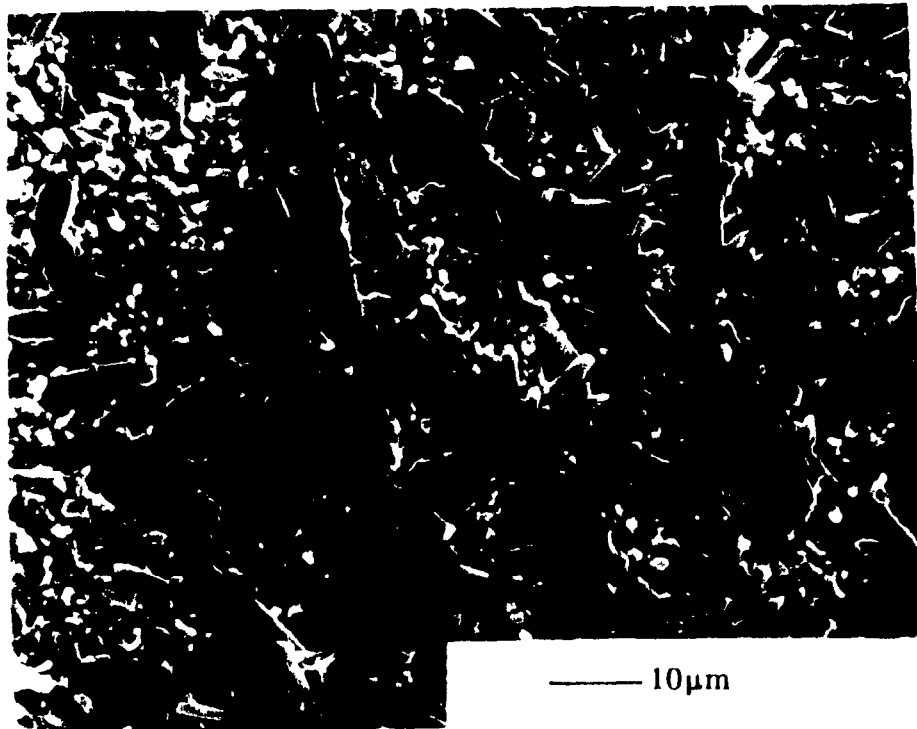


Fig. 5.9: Polished surface of Si_3N_4 with 5% whiskers (NaOH etch).

discussed further in 5.2 below). Many authors have shown that the strength and relatively high toughness of Si_3N_4 is attributed to the fact that its microstructure consists of acicular grains⁽¹⁰⁶⁾. There have been several attempts at finding the optimum aspect ratios of these grains, with respect to mechanical properties⁽¹⁰⁷⁾, and increasing the aspect ratio appears to improve these properties as a result of inhibiting propagation of cracks. From the microstructure shown in Fig. 5.9, it appears that this could be a suitable method of improving the properties of Si_3N_4 , provided there were enough acicular grains in the matrix, and that the material is close to full density.

The use of external pressure during sintering is one solution to this problem and, indeed, this has been shown to be an effective way to obtain enhanced mechanical properties of the material⁽⁹¹⁾. However, as mentioned in section 2.1.4.2, this method is not viable for producing components at a reasonable price, due to the complexity of the equipment. In this case, the capillary pressure created by the liquid phase was not enough to overcome the bridging effect of these whiskers. To minimize this, and in an attempt to improve densification, the whiskers were characterized and to some extent modified.

5.1.3 WHISKER CHARACTERIZATION

A sedimentation technique was used to separate any large whisker particulates or hard agglomerates. The pH of the suspension was raised to >9.0 and after stirring, the particles were left to settle. The bottom layer of the suspension was discarded. A

sample of whiskers taken from this layer (Fig. 5.10) shows the large whiskers and whisker agglomerates found. The remaining whiskers were dried and mixed with powder, in a manner described previously, and the sintered densities of these samples were found to be about 3% higher than the ones using as-received whiskers.

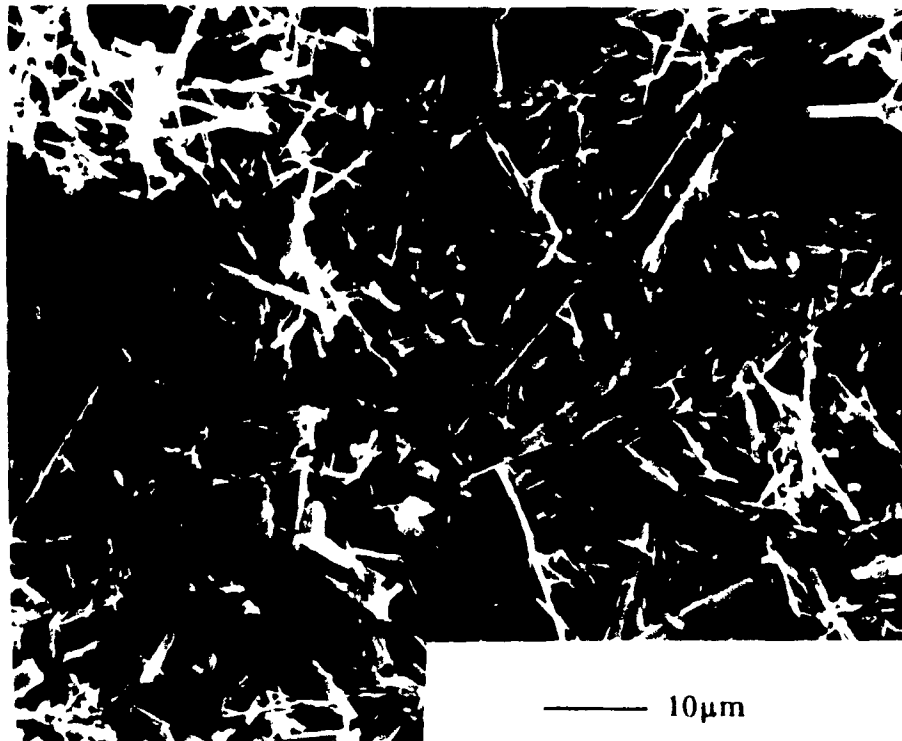


Fig. 5.10: Sample of whiskers separated from the as-received batch.

Reducing the length of the whiskers would also lessen the chances that whiskers bridge on one another. Fig. 5.11 shows whiskers which were attrition milled for 2 hours in iso-propyl alcohol. Their aspect ratio was reduced from the 15-50 (as-received) down to 5-35. When these whiskers were added to powder and sintered, the density increased to 90%, a 5% improvement. No further increase in density was noted when these milled whiskers were separated in the manner described above.

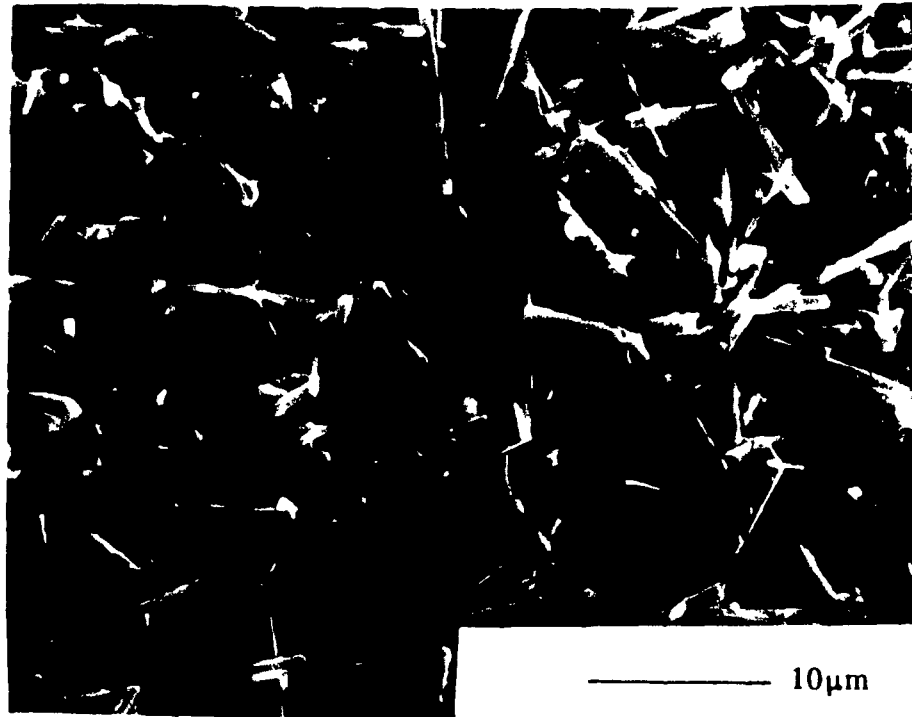


Fig. 5.11: Whiskers after 2 hours of attrition milling (Aspect Ratio=5-35).

5.1.4 MECHANICAL PROPERTIES

Bars of varying whisker content made using the different dispersion methods were tested in 4-point bending and the values obtained are shown in Fig. 5.12. It is clear that as the whisker content of the samples increases, the strength decreases irrespective of their preparation method. However, it should be noted that the density of the samples also decreased, as shown in Fig. 5.2. What is noticeable from the graph is the fact that at any whisker loading, the milling/sonication method yields better strengths. One possible explanation for this could be the fact that by using hydromechanical forces, all the different powder agglomerates are broken down and

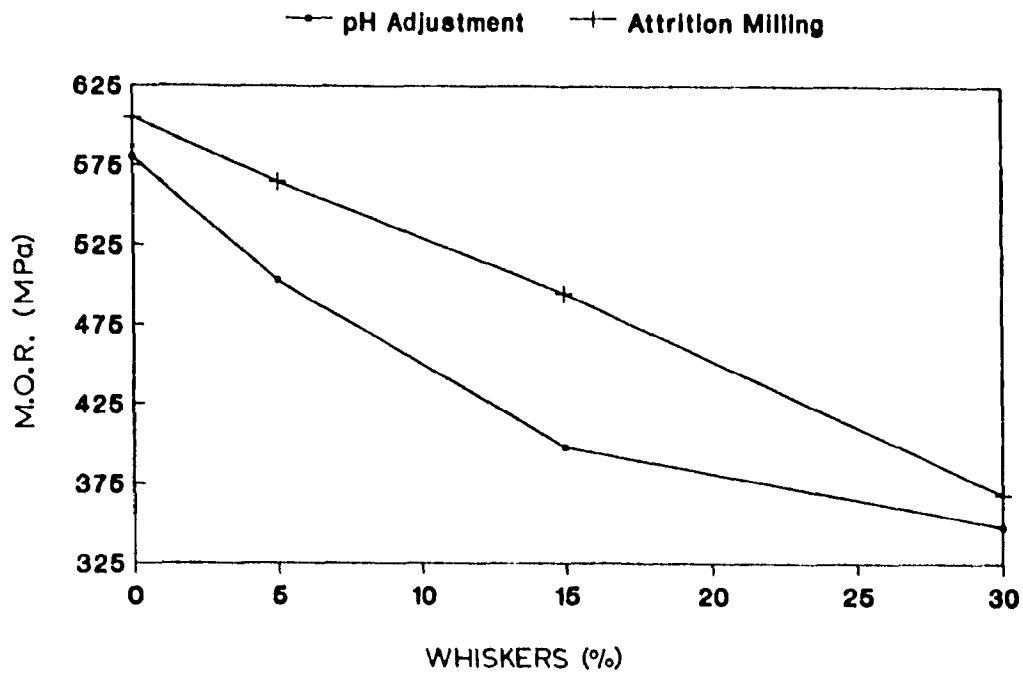


Fig. 5.12: M.O.R. values vs. whisker content.

dispersed. In addition, it may be possible that the pH adjustment method, whilst stabilizing the Si_3N_4 powder and whiskers, may not provide the correct conditions for dispersing the various sintering additives, in particular the oxides Al_2O_3 and Y_2O_3 ; indeed Al_2O_3 is usually dispersed at a pH of 3-4⁽⁸²⁾. This could possibly have resulted in localized inhomogeneous regions which may have caused fracture. The attrition milling method, by contrast, gives a good distribution of the sintering additives⁽⁷⁸⁾ and this would have improved the sintering behaviour and hence the mechanical properties of the material.

5.2 EXTRUSION

It has been seen that whisker bridging, and the resulting skeletal network inhibit densification and it is believed that these whiskers do not break down during the sintering process. A possible solution to this problem is to align the whiskers, such that during densification they would not impinge on one another, forming interlocking bridges.

Whisker alignment has previously been reported in work involving injection molding of ceramic pastes⁽¹⁰⁸⁾. The processes of injection moulding and extrusion were therefore obvious choices to purposely achieve such an effect. Extrusion, being the simpler of the two processes, was chosen for the present work. Extrusion of ceramic pastes is not new in fabricating ceramics⁽¹⁰⁹⁾, indeed, many components, for traditional and advanced ceramics, are produced in this way. However, the use of this method to form ceramic composites is a relatively new concept. The alignment of the whiskers is achieved by the use of a plasticizer, which transforms the powder into paste. The properties of this paste differs from that of a conventional one used to produce extruded parts. Normally, the material consists of powders containing a wax, clay or low-molecular-weight polymer which are sufficient to bind the powder together, provide the lubrication for flow to occur easily through the nozzle and allow for quick and clean burn out⁽¹¹⁰⁾. In the extrusion of a powder/whisker mixture, however, maximum polymer-whisker interaction is desired to produce the necessary alignment.

A cellulose based polymer, or more specifically, Hydroxypropyl Cellulose (HPC) was used as the plasticizer in the present work^(100,101). The molecular structure is shown in Fig. 5.13. The choice of such a plasticizer is attributed to the fact that this polymer has a large molecular weight (300,000) and the chain is in the form of a coil. This was suggested to be beneficial in aligning whiskers, as shown schematically in Fig. 5.14⁽¹¹¹⁾. The polymer chains are known to stretch and align themselves upon the action of shearing. The attachment of the chains onto the whiskers would thus promote alignment of the whiskers.

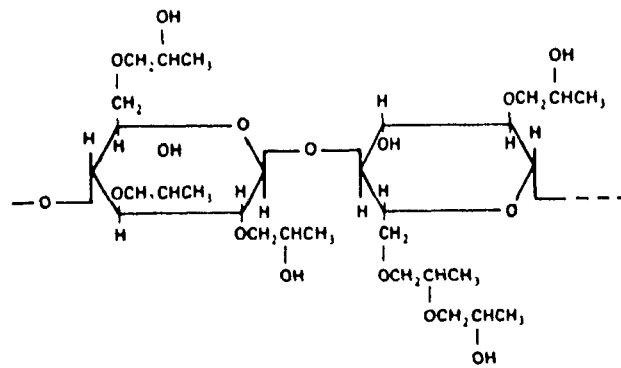


Fig. 5.13: The HPC molecule.

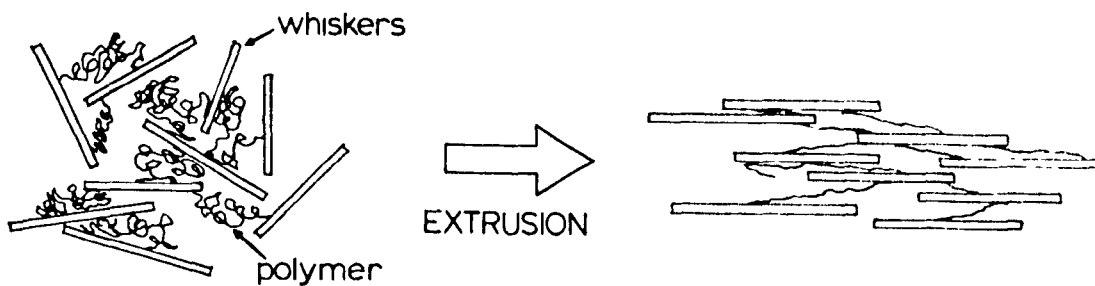


Fig. 5.14: Schematic of polymer/whisker interaction.

As already mentioned in section 4.4.2, this plasticizer is soluble in water. The ratio of water : HPC : powder is a critical factor in the formation of a semi-solid extrudable paste. A good working ratio was found to be (15ml water):(1g HPC):(26g powder).

5.2.1 SAMPLE FABRICATION

The resulting paste had a viscosity low enough for shearing to occur, this being provided by the reduction in nozzle diameter and friction with the walls of the extruder, yet high enough to retain its shape on exit through the nozzle. Upon sintering, the density was measured to be 91.5% for a 15% whisker content. This is a substantial improvement over the 85% density obtained for an isotropically dispersed, pressed whisker composite. Control tests, to see whether full theoretical density could be obtained using this extrusion method, were performed with samples having 0% and 10% whisker content. The 10% whisker composite samples had sintered densities of 95% and the sample with no whiskers had a density in the range 97-98%. This implied that the plasticizer being used did not affect the sintering of the material itself. The resulting porosity that was found in the 15% whisker samples was mostly due to the presence of the whiskers, as will be seen later.

The fact that a higher density was achieved indicated that the idea of aligning whiskers to reduce whisker bridging was somewhat successful. Furthermore, the use of HPC as a plasticizer appeared promising. When compared to another commercial

cellulose, namely Methyl Cellulose (M.W. 3,000), the highest density obtained for samples prepared under the same conditions was only 89%, for a composite having 15% whisker content.

It became apparent that water content was a critical factor in the formation of macro-porosity in the green state, especially during the drying stage after extrusion. The extrudate was dried at a very slow rate by being left at room temperature overnight to minimize the formation or expansion of bubbles, resulting from water attempting to leave the extrudate by vapourizing too fast.

Indeed it was seen that water content did effect the final sintered density of the material. By increasing the amount of water in which the plasticizer was dissolved, and hence the water content of the paste, sintered densities decreased steadily to a value comparable to that obtained for pressed whisker composites, i.e. 85% (Fig 5.15). In fact the paste with the highest water content had such a low viscosity upon exit, it did not retain its cylindrical shape as an extrudate. Since the paste was able to flow freely, the whiskers lost all form of alignment.

It is obvious that certain parameters must be controlled to obtain a suitable paste for extrusion, the most important one being mixing. As mentioned in section 4.4.2, the powder, after granulation, was incorporated into the dissolved plasticizer. Mixing was done manually, so there was no real guarantee that all the powder was being mixed in, or conversely, the plasticizer was not coating every particle, which at that stage was in the form of soft agglomerates (as a result of granulating through a 212 μ m mesh). Therefore the paste had to be kneaded after mixing. This was done by extruding

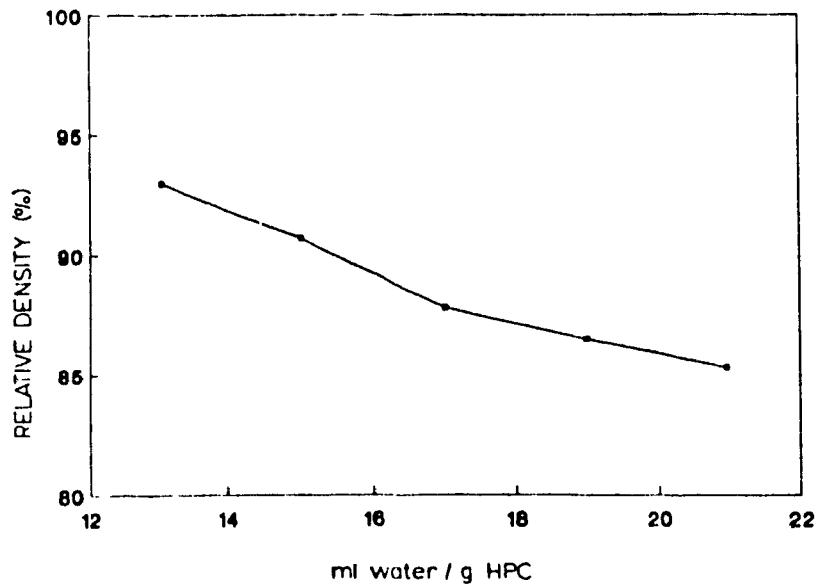


Fig. 5.15: Sintered density vs. water content in extrudate.

the same paste twice. The shearing action resulted in better mixing and yielded an improvement in sintered density from an average of 91.5% up to an average of 92.5%. All values discussed so far were for powder/water mixtures dispersed using pH adjustment; i.e. the method which gave higher green density values for pressed bars (section 5.1). When a batch of powder was prepared under the optimized conditions as described but using attrition milling and ultrasonic dispersion, the average sintered density of the extruded samples was 94.5% with some values even reaching 96.5%.

A variety of nozzles were used throughout. The first nozzle diameter was of 5mm diameter and when increased to 8mm, the sintered density was the same. However when a square-sectioned nozzle of 10mm was used, the sintered density of the

extrudate dropped to 91%. This suggested that the nozzle opening was too large for the shearing force to align the whiskers in the centre of the extrudate (i.e. plug flow was occurring). The inclusion of a *spider* (an insert in the nozzle opening, as shown in Fig. 5.16) solved this problem. In fact the highest sintered densities of 95% were achieved

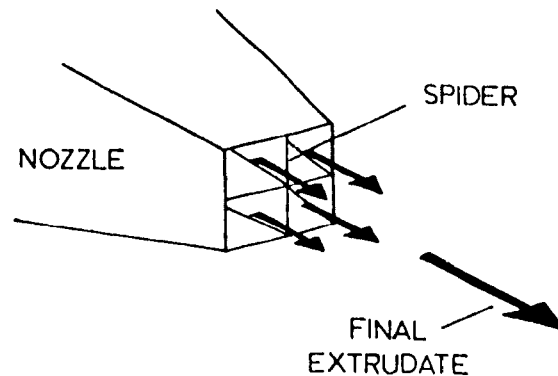


Fig. 5.16: The inclusion of a spider in the nozzle.

for samples initially extruded through the 8mm circular nozzle, then extruded again through the square sectioned nozzle containing the spider.

Porosity was a constant problem in this work, be it in the matrix or on the extrudate surface. To study the formation of the surface pores, samples were extruded using only Si_3N_4 powder. After burn-out of the polymer, a study of the cross-section of a powder compact revealed large pores (Fig. 5.17), ranging in size from $50\mu\text{m}$ up to $150\mu\text{m}$. These are thought to be due to air pockets trapped in the paste during mixing, mainly because of their smooth and spherical shape. This implies that they were probably formed when water was still present. They are not the result of burn-out of the polymer, primarily because of their large size, and secondly because of their

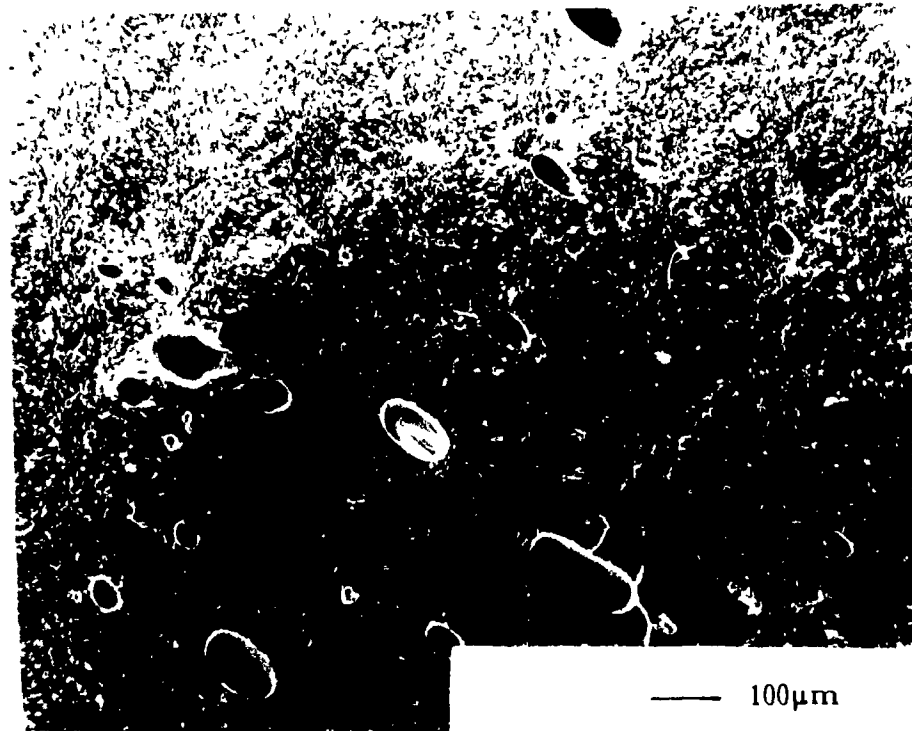


Fig. 5.17: Fracture surface of green compact after burn-out (no whiskers).

smooth shape; a burn-out pore would have a much more irregular shape. Upon cold isostatically pressing bars, these pores appear to have been forced out from the centre of the sample to the surface, coalescing in the process to form large (500µm-1mm) surface pores and irregularities. To eliminate these pores, the paste was extruded through a fine mesh, into a vacuum chamber. This produced a better extrudate with improved surface features. A fractured surface of this extrudate, having 15% whisker content, after burn-out is shown in Fig. 5.18. Although some pores are still evident, the number is far less for the vacuum/fine mesh extrudate (Fig. 5.19). It was seen that the vacuum did prevent porosity resulting from entrapped air. This approach to obtain a denser green compact has been successfully applied in the clay industry for many

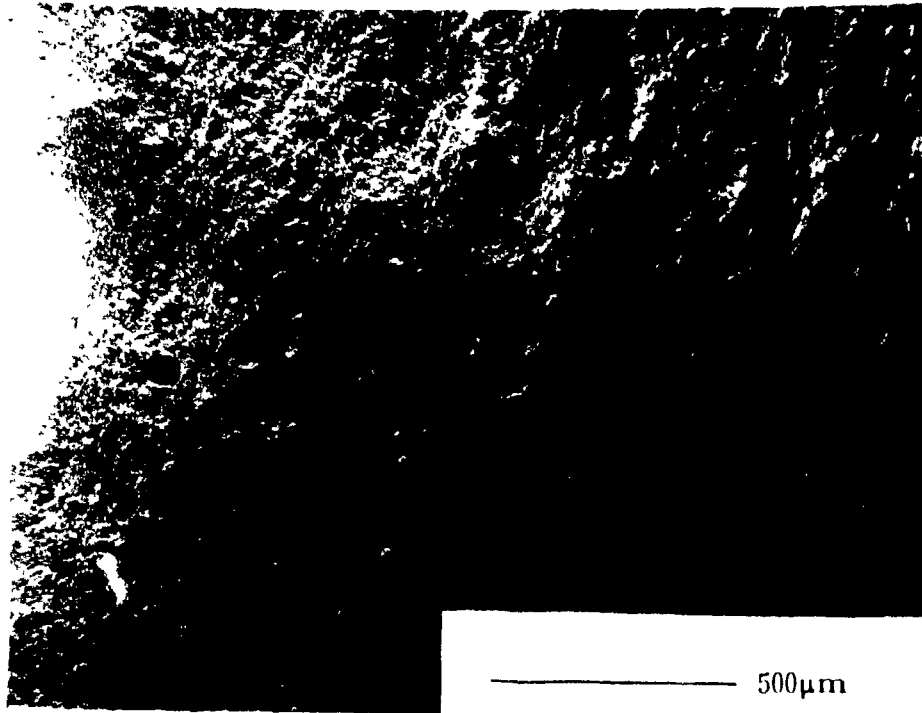


Fig. 5.18: Fracture surface of green compact after burn-out extruded through mesh into a vacuum (15% whiskers).



Fig. 5.19: Fracture surface of green compact extruded under standard conditions, after burn-out (15% whiskers).

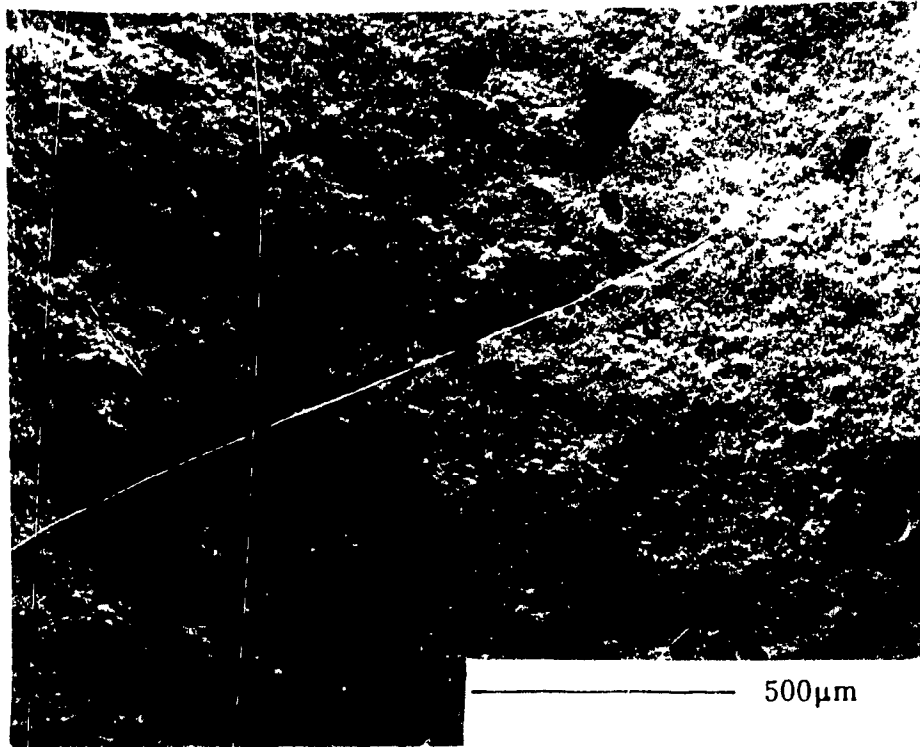


Fig. 5.20: Fracture surface of green extrudate mixed using mechanical mixing, after burn-out (15% whiskers).

years, and is called *pugging*⁽¹¹²⁾.

The use of a mechanical mixer to mix the plasticizer and powder aggravates the problem by incorporating numerous air bubbles. A cross-section of this sample after burn-out (Fig. 5.20) reveals many more air pockets than those found in Fig. 5.18 and 5.19. Although this method seems to produce a more uniform paste, it entraps more bubbles. A possible solution may be to perform the mixing under a vacuum. This however introduces problems with drying out of the paste due to water removal.

5.2.2 SHRINKAGE

The densified extruded samples had different shrinkage behaviour to that of

pressed samples not containing whiskers. Whereas, for monolithic material with 96-98% density, there is an isotropic linear shrinkage of about 18%, the extruded bars yielded a linear shrinkage of only 6% in the direction of flow of the extrudate, but 24% in the other two transverse directions, as shown schemetically in Fig. 5.21. This lends further evidence to the belief that the whiskers are being aligned, thus allowing greater shrinkage in a direction perpendicular to the direction of the whiskers. Similar shrinkage behaviour has been reported in other work dealing with slip cast samples, where values of 7% and 21% linear shrinkage were quoted for the same respective directions⁽⁸⁵⁾.

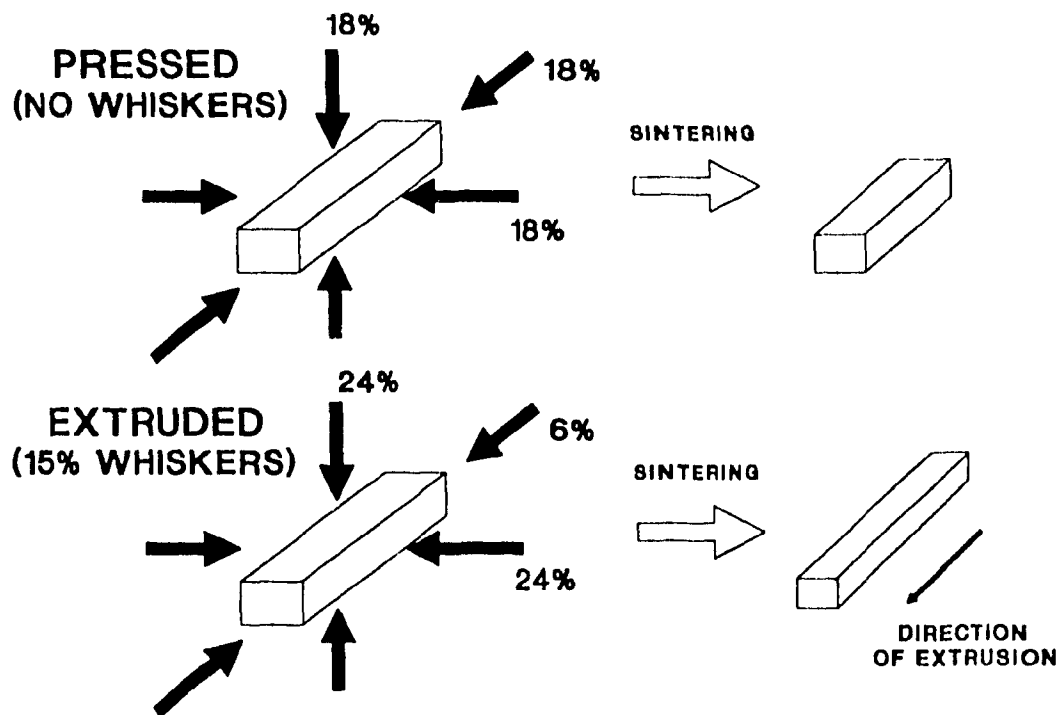


Fig. 5.21: Isotropic shrinkage of pressed samples versus anisotropic shrinkage of extruded samples containing whiskers.

5.2.3 MICROSTRUCTURAL EXAMINATION AND DENSIFICATION

Analysis of a cross-section of the green extrudate clearly showed the alignment of the whiskers (Fig. 5.22) and also showed that whisker dispersion was achieved. However some areas appeared more random and unaligned, but it is not clear whether this is due to bad dispersion, insufficient shearing, or simply from the action of fracturing the green body. Further analysis revealed that these whiskers retained their alignment even in the transformed sintered microstructure, giving a matrix having elongated β -grains in one direction, in a matrix of β -crystals (Fig. 5.23).

The size and aspect ratio of the whiskers in the sintered material changed, as was also observed in the pressed whisker composites discussed in section 5.1 above. Table 5.1 compares the measured dimensions of the original whiskers with the large crystals remaining in the sintered microstructure, for both the extruded and pressed samples. By comparing the values in Table 5.1, it appears that there is only a minor change in the length of the whiskers upon sintering, in both the extruded and pressed samples. On the other hand, their diameter seems to have doubled, and consequently, their aspect ratio decreased to half the original value. Indeed these grains must be growing during the transformation process. Since the liquid phase is also wetting the whiskers during sintering, it is possible for the β Si_3N_4 to be precipitating from the liquid phase onto the whiskers rather than forming new grains (as is the case during sintering of monolithic Si_3N_4). This observation may also be confirmed by comparing Fig. 5.23 to 5.9 and to the original whiskers shown in Fig. 4.1. Furthermore the

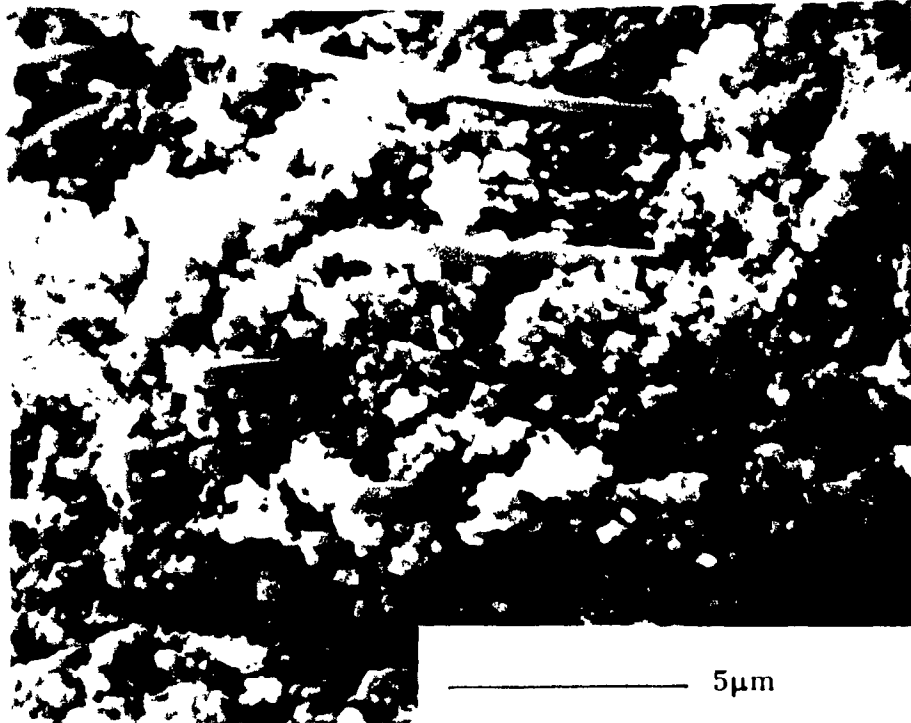


Fig. 5.22: Green extrudate showing whisker alignment (15% whiskers).

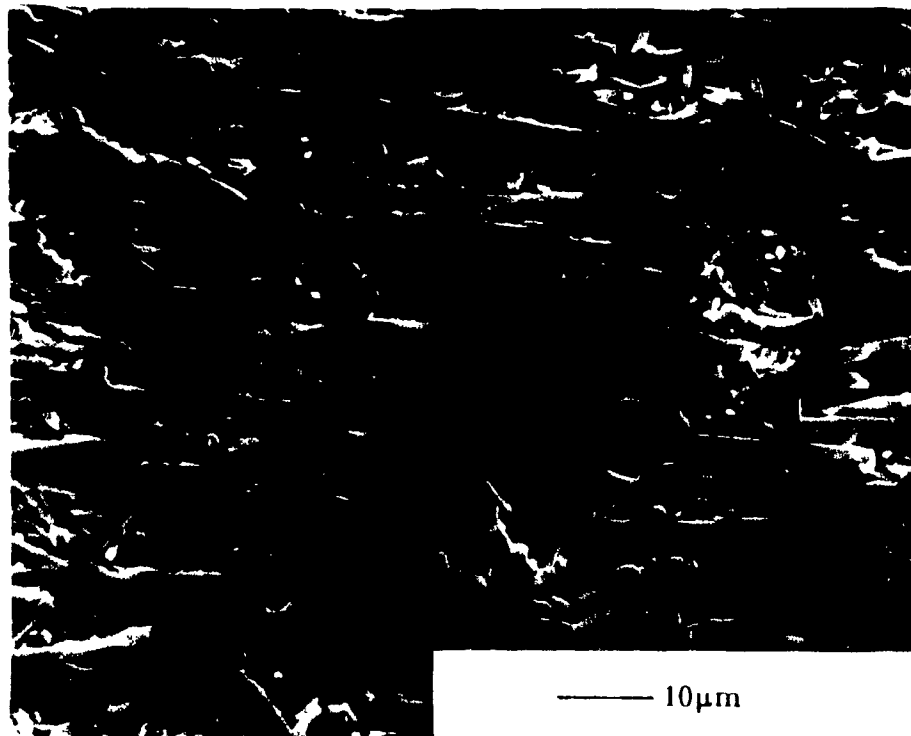


Fig. 5.23: Polished sintered extrudated showing alignment (NaOH etch).

Table 5.1: Comparison of size and A.R. for whiskers before and after sintering.

	WHISKERS	LARGE β CRYSTALS	
	AS-RECEIVED	EXTRUDED	PRESSED
LENGTH (μm): AVG. RANGE	20 10-40	24.6 10-35	22 12-35
DIAMETER (μm): AVG. RANGE	1.11 0.3-2.5	2.13 1-4.5	2.41 1-3.5
ASPECT RATIO (μm): AVG. RANGE	18 7.5-85	11.5 6.66-20	9.1 7.5-12

microstructure in Fig. 5.23 shows that there is actually more than 15% by volume of directional acicular grains in the material (the matrix seems to have a much more acicular nature than that of a monolithic material, as shown in Fig. 5.24). The suggestion is that some of the transformed crystals are growing in a preferred

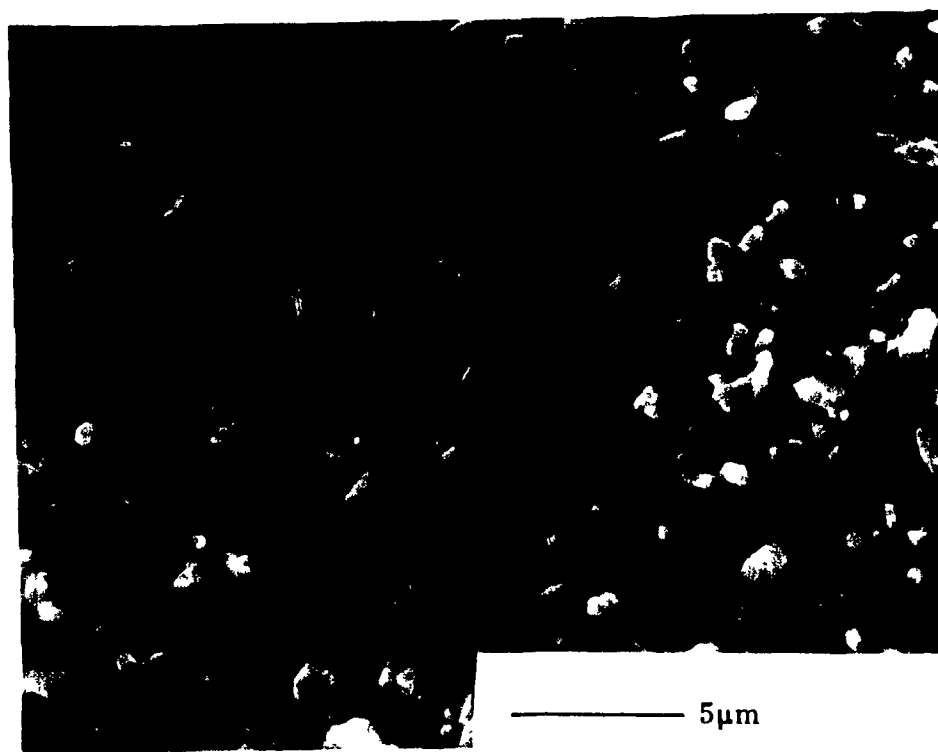


Fig. 5.24: Microstructure of monolithic Si_3N_4 .

orientation, i.e. in the direction of alignment. This may be a result of the anisotropic shrinkage behavior of the material. Because there is a higher percentage of powder in a transverse direction, shrinkage is greater and less restrained. The different sintering pressures are creating similar conditions as that of hot-pressing, where preferential grain growth is also observed. In hot-pressing, new grains find it easier to grow in a direction perpendicular to the applied force, with material precipitating at the tips of the grain, rather than in a direction opposing the force. Similarly, in the aligned whisker composite, the same mechanism could possibly be operating, as seen in Fig. 5.25, where small acicular grains are found growing between the larger β crystals. Fig. 5.26 is a schematic which summarizes the two proposed sintering mechanisms involved. Upon sintering the extrudate, having aligned whiskers in a powder compact, a liquid

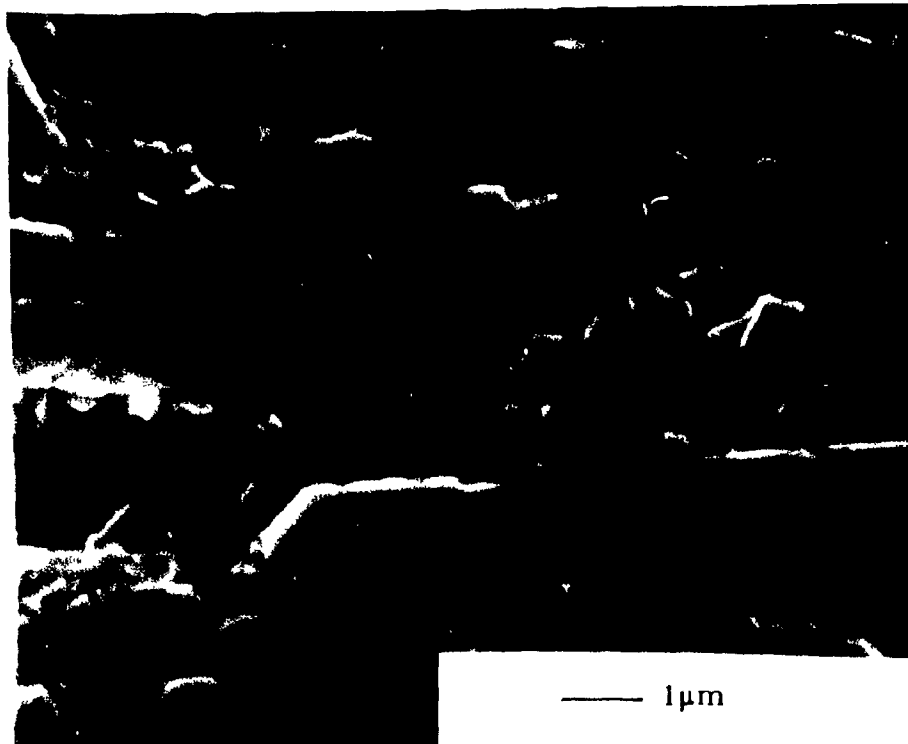


Fig. 5.25: Sintered extruded sample showing preferred grain growth.

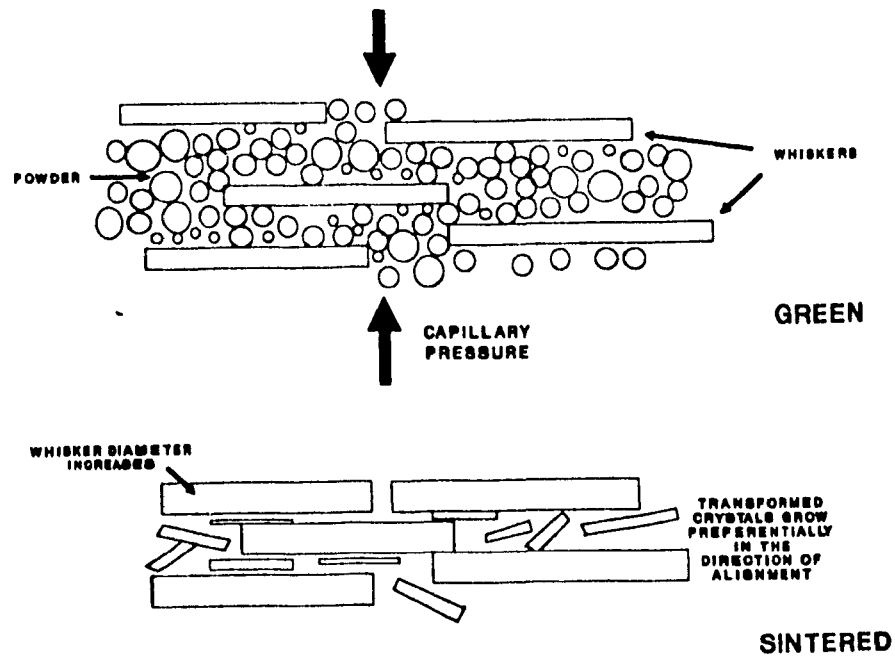


Fig. 5.26: Schematic of the sintering of aligned whisker composites.

phase forms and the matrix shrinks. The α powder then goes into solution and β Si_3N_4 reprecipitates on either the original whiskers or in the form of new grains, which grow preferentially in the direction of the alignment.

Another feature in the microstructure of the sintered material is the presence of "white" regions. These spots were analysed to be areas of lower density with little or no alignment of whiskers apparent (Fig. 5.27). There are two possible explanations for the occurrence of these regions:

a) large pores formed during extrusion collapsing during isostatic pressing, to cause a disorder in the alignment pattern of the whiskers (the size of these regions is comparable to that of the large pores resulting from bubbles during mixing, discussed

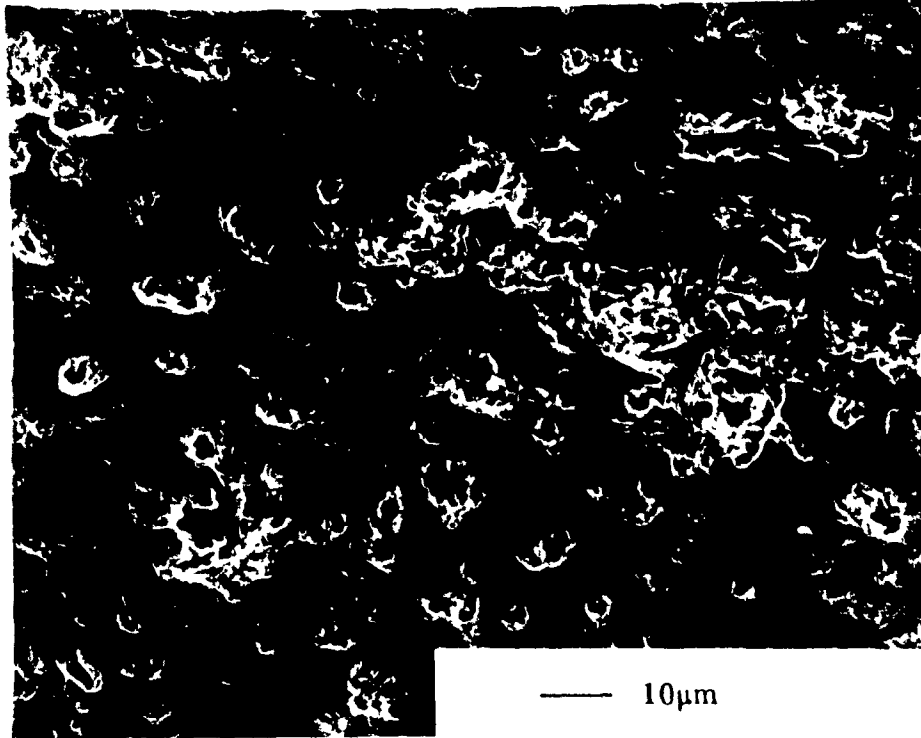


Fig. 5.27: A region of low density, probably a white spot in a polished sintered extrudate (15% whiskers), etched with IIF.

above). Thus the region would not fully densify due to the whisker bridging effect found in unaligned material as described in section 5.1.2.

b) powder agglomerates formed during the drying and granulation stage of the processing. These did not break down during the mixing with the polymer or during the shearing action of extrusion and thus sintered in a different manner to the rest of the matrix. This problem of differential sintering of agglomerates is well documented⁽⁷¹⁾, and is often the cause of low porosity regions similar to those observed as "white spots" in this material.

As further support of the above, a cross-section of a green extrudate, having

15% whisker content was examined after isostatic pressing (Fig. 5.28). The fractured plane was perpendicular to the direction of the principle whisker alignment. The sample revealed areas in the microstructure where whiskers seemed to be flowing in various directions.

To trace the source of these defects, the powder/whisker mixture and plasticizer were examined. Some dried, granulated powder was mixed into a large quantity of plasticizer (to allow easier observation), and a small sample was placed in between two glass plates and viewed with an optical microscope using transmitted light. As shown in Fig. 5.29, the mixed paste contains dispersed whiskers and powder, plus air bubbles (A) and agglomerates (the dark irregular shapes, B). The agglomerates were identified by applying a severe shearing force between the plates and observing

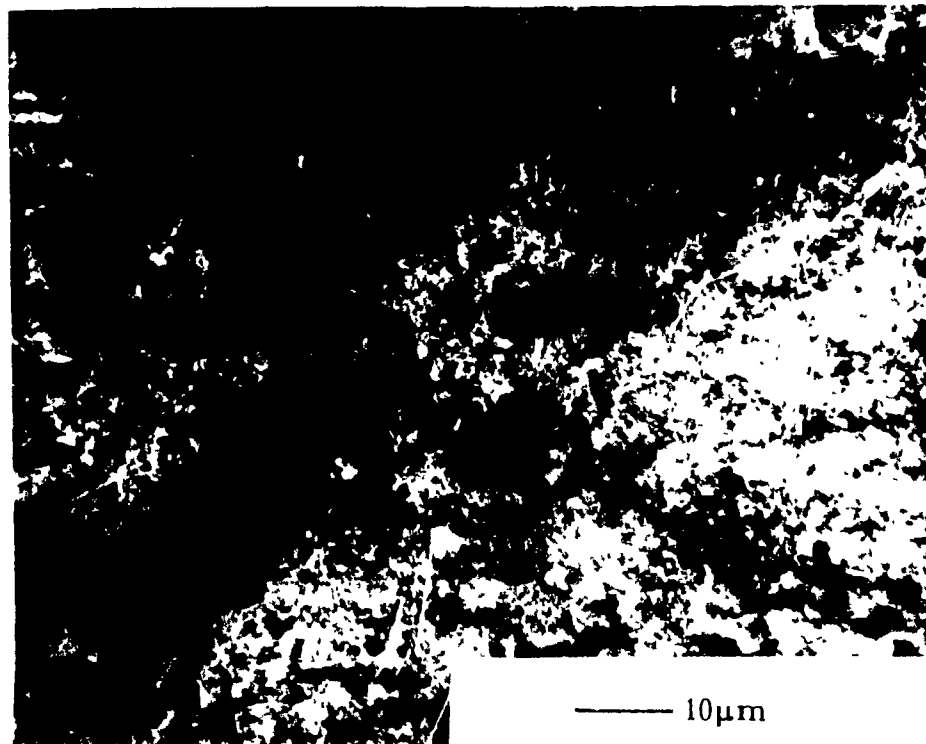


Fig. 5.28: fracture surface of C.I.P. sample, showing misalignment.

their break-down into whiskers and powder as seen in Fig. 5.30. This shows that manual mixing is not sufficient to completely disperse the powder, i.e. the resulting mixture still contained large agglomerates. These are the same agglomerates that are presumed to result in a non-aligned region, as shown in Fig. 5.26. The presence of the bubbles emphasises the problem of entrapped air, which is bound to result with any form of mixing carried out at atmospheric pressure. The paste was subjected to further mechanical mixing, to see whether increasing the shearing action during mixing would disperse these agglomerates. Most of them remained intact, however there was a drastic increase in the number of air bubbles present in the paste as shown in Fig. 5.31, and further shows the undesirable effect mechanical mixing may have on this plasticizer, as was already described in Fig. 5.20.

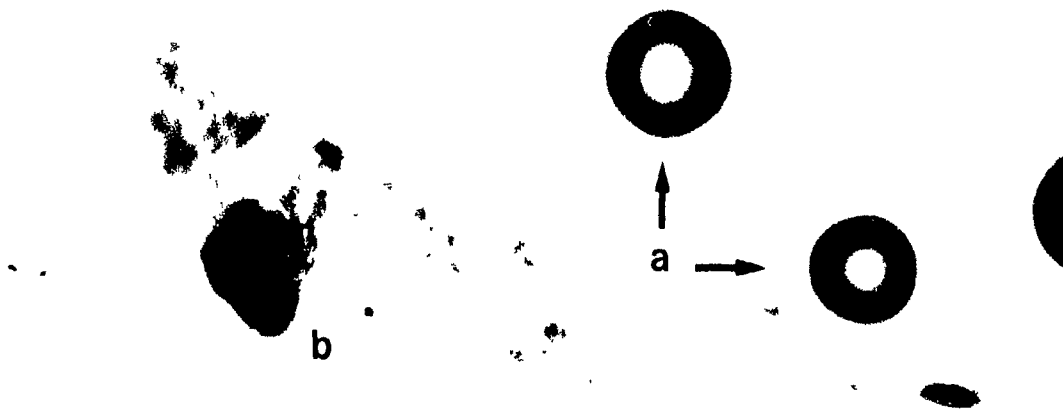


Fig. 5.29: optical micrograph of agglomerates remaining in the paste (x100).

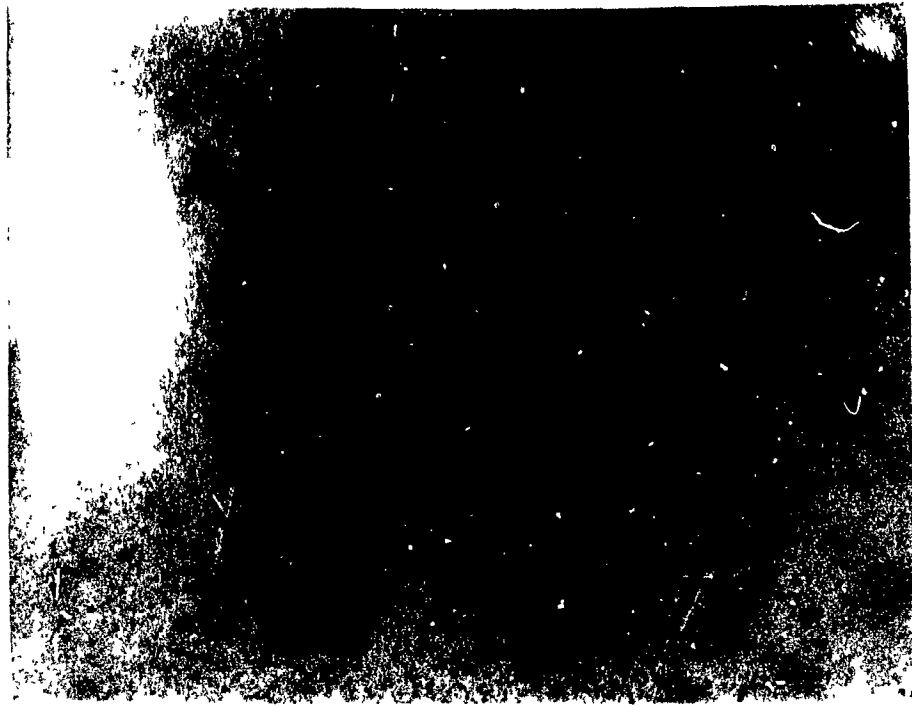


Fig. 5.30: The agglomerates after being broken up by shearing (x100).

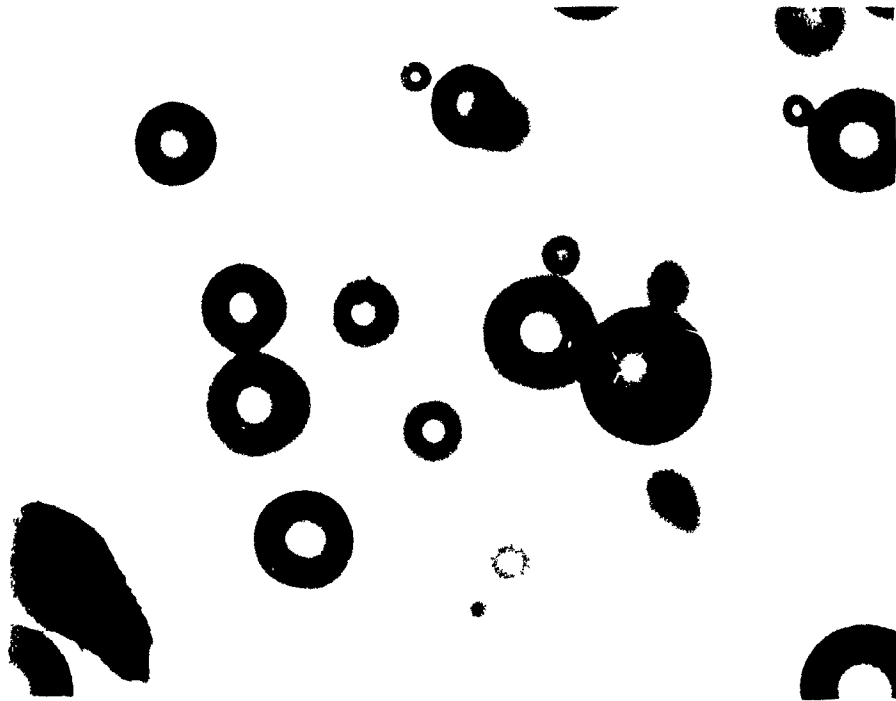


Fig. 5.31: optical micrograph of the paste after being mixed mechanically (x100).

5.2.4 MECHANICAL PROPERTIES

The Modulus of Rupture (M.O.R.) values for the high density samples (95% relative density) were low when compared to values obtained for monolithic material. The average strength for twelve samples was 276MPa, all lying within the range 243-357MPa, compared to 700MPa for monolithic material. Analysis of the fracture surfaces showed that the critical defects were mostly large surface pores (of the order of 200 μ m) at the edges of the sample (Fig. 5.32), the origin of these pores being associated with air bubbles, as discussed above.

The material, as expected, exhibited different toughening behavior in directions parallel and perpendicular to the reinforcing phase. Fig. 5.33 is a typical indent on a

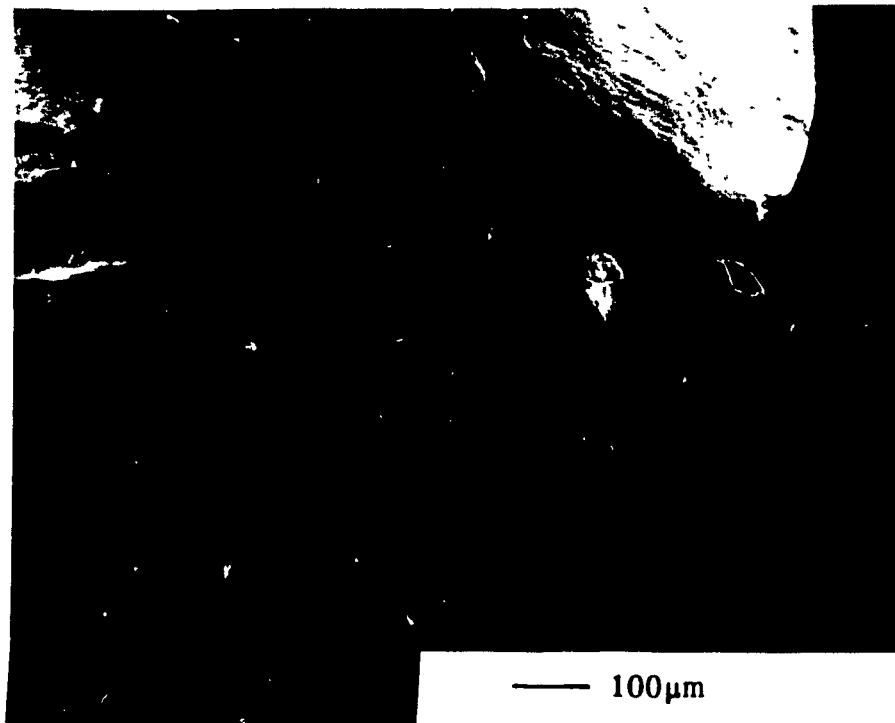


Fig. 5.32: Fracture origin of M.O.R. test sample.

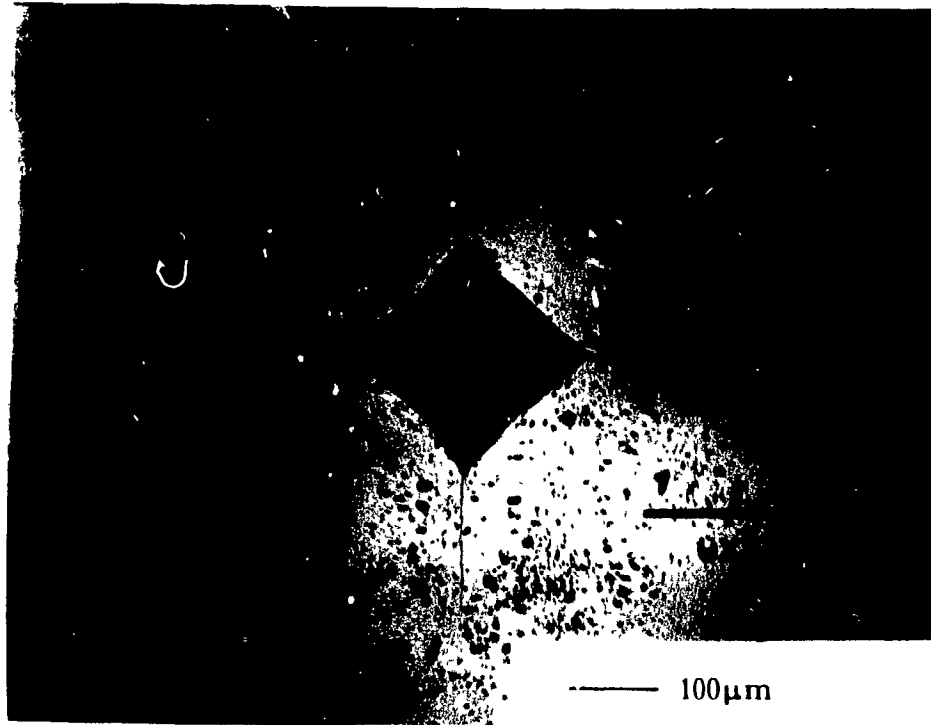


Fig. 5.33: Optical micrograph of a Vicker's indent to measure toughness.

polished surface of the material. It is very obvious that the crack lengths in the two directions are of different lengths, the crack running perpendicular to the reinforcement being approximately half the size of the other. Table 5.2 lists the average values of K_{Ic} for the two directions tested on four different specimens and a control specimen of monolithic Si_3N_4 .

The fracture toughness values measured perpendicular to the reinforcement direction are consistently higher than those measured parallel to the whiskers. However there is a large spread in the range of these values, from 7.0 to 13.5 $\text{MPa}\cdot\text{m}^{1/2}$ in the perpendicular direction and 3.3 to 8.5 $\text{MPa}\cdot\text{m}^{1/2}$ in the parallel direction. A plausible explanation for these variations is the fact that the indent, although aligned with

Table 5.2: Toughness values for a 15% whisker-reinforced extrudate.

SAMPLE	PERPENDICULAR (MPa.m ^{1/2})	PARALLEL (MPa.m ^{1/2})	NO. OF INDENTS
Si ₃ N ₄	8.2±0.7	8.1±1.3	4
A	13.0±1.2	8.5±0.8	5
B	7.6±2.1	3.3±0.8	13
C	7.0±1.2	4.2±0.9	10
D	13.5±2.2	4.6±1.0	14

respect to the sample edge, may not have been perfectly aligned with the whiskers. In addition, these samples had ~5% porosity in the matrix, as may be seen in Fig. 5.33, and this may effect crack propagation behaviour.

The cracks produced by the indents were examined using SEM to establish the method of crack propagation. The cracks running along the direction of reinforcement were *intergranular*, and propagated quite easily through the grain boundary phase (hence the lower value), as shown in Fig. 5.34. On the other hand, the cracks running perpendicular to the reinforcement were mostly *transgranular* (Fig. 5.35), even though the crack path appears to be quite rugged, and with some crack branching (Fig. 5.36). The fact that the perpendicular cracks propagated through grains rather than around them may be explained by the fact that more energy is required to fracture around the grain than across the crystal. Thus the crack preferentially cleaves through the crystals. However, since it has to propagate across numerous grain boundary/matrix interfaces, the crack loses considerable energy in reinitiating fracture before cleaving again, resulting in an increase in K_{Ic} .

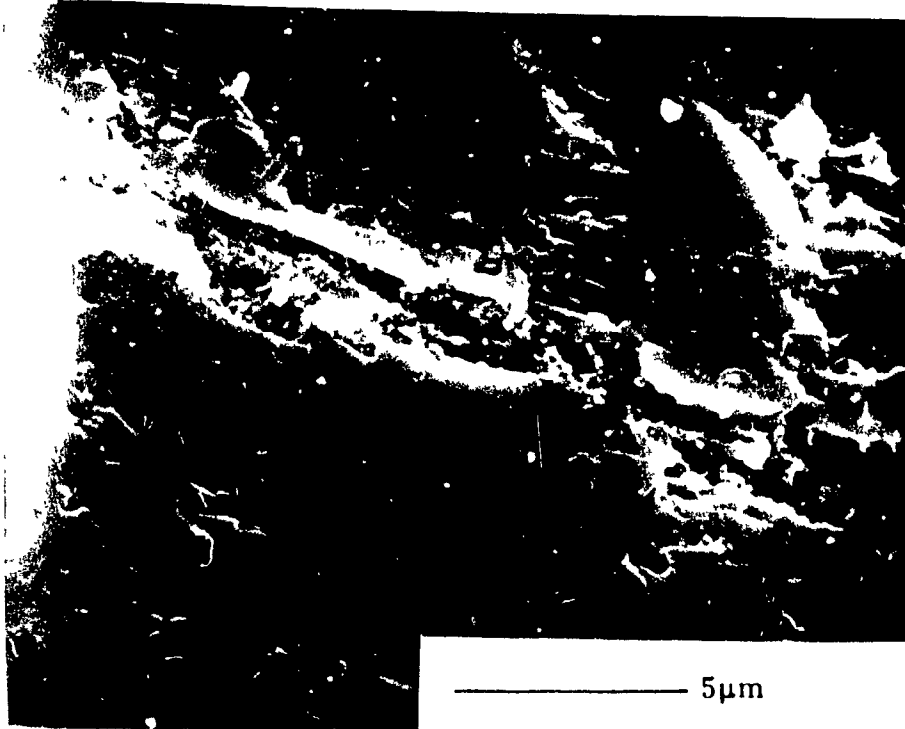


Fig. 5.34: Intergranular fracture along the reinforcement.

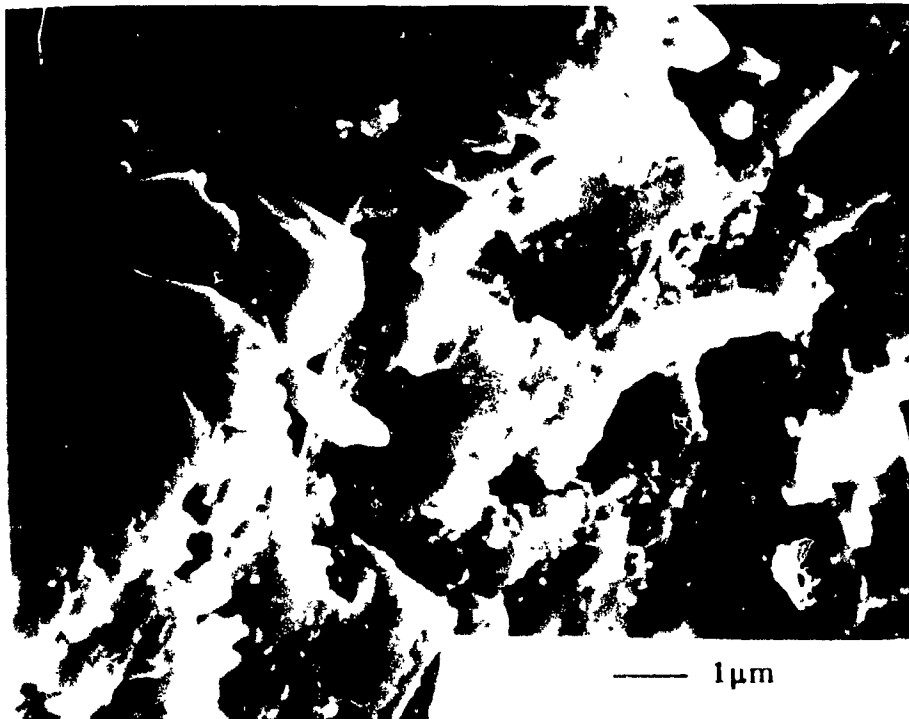


Fig. 5.35: Transgranular fracture across reinforcement.

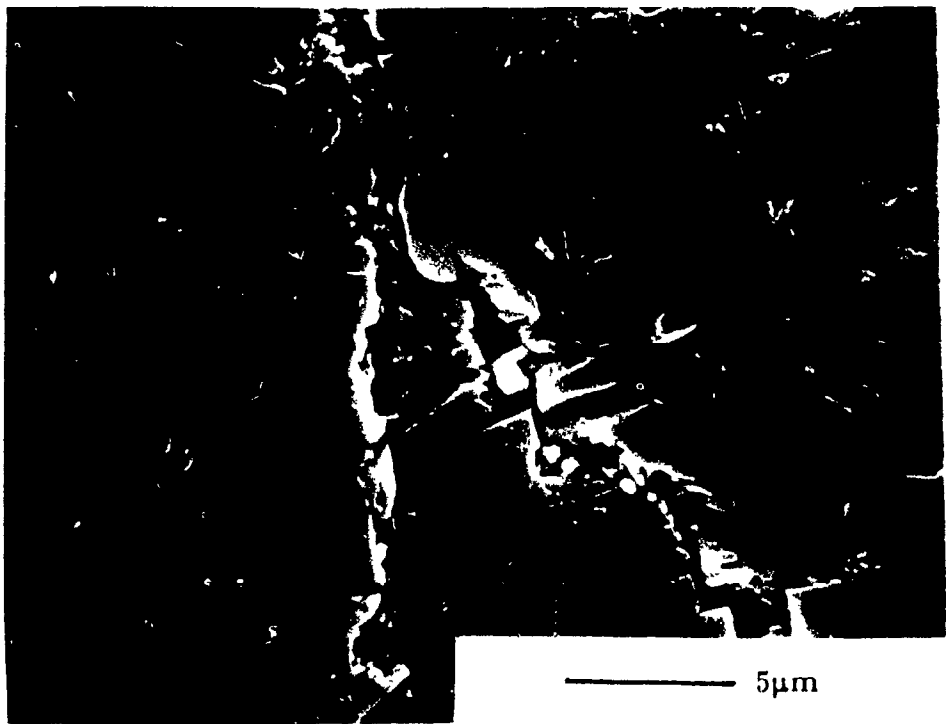


Fig. 5.36: Branching, and deflection of the crack.

6. CONCLUSIONS

1. Densification of whisker-reinforced Si_3N_4 using pressureless sintering is hindered by the presence of whiskers, which form an interlocking network inhibiting shrinkage. The liquid phase did not seem to provide enough lubrication to aid the rearrangement of particles, nor was the capillary pressure large enough to overcome the bridging of the whiskers. Removing the larger particulates and reducing the aspect ratio of the whiskers minimize whisker bridging and lead to an increase in the sintered densities.

2. By aligning the whiskers it was possible to obtain high densities of ~95% using pressureless sintering. Shrinkage of this material was highly anisotropic. An extrusion process was developed to achieve this and the use of a plasticizer, namely Hydroxypropyl Cellulose, helped to achieve alignment of the whiskers.

3. The extrusion process was sensitive to a number of variables:

i) The water content must be minimal, yet high enough to provide the lubricating medium necessary for the polymer to operate in.

ii) It was shown that good powder/plasticizer mixing is essential. Extruding the paste twice helps knead the paste and improves mixing. All soft agglomerates should be broken down into loose powder, such that all whiskers may be aligned. This was seen to be a problem in this work, and resulted in porosity in the microstructure. However, mixing should not be too aggressive as this seems to increase the amount of entrapped

air in the paste. These air pockets created problems in the green microstructure, which coalesce to become large surface pores upon pressing, and can create misalignment of the whiskers as a result of their cavitation. The number of air bubbles seemed to decrease when the paste was extruded through a fine mesh into a vacuum chamber. This appears to be a promising way of obtaining better green bars.

iii) The green and sintered microstructures revealed alignment across all of the sample. The whiskers increased in diameter and decreased in aspect ratio on sintering; and the transformed crystals grew in a preferred direction parallel to the reinforcement. White spots visible in the matrix were analysed to be areas of low density, with little or no alignment. These were probably caused by the soft agglomerates and/or the cavitation of pores.

4. M.O.R. values were low compared to monolithic materials. Fracture initiated at surface porosity present on the sides of the test specimen. The elimination of the low density regions would probably increase the strength. The toughness values, on the other hand looked promising. The material had anisotropic values, those in a direction perpendicular to the reinforcement being at least twice those parallel to it. High toughness values were obtained in general, sometimes being twice that of a monolithic material. The cracks were analysed to be transgranular in the perpendicular direction and intergranular in the other. These results confirmed that it is possible to reinforce Si_3N_4 by Si_3N_4 whiskers and that extrusion and pressureless sintering may be used to obtain an anisotropic composite having high sintered density and good toughness.

7. SUGGESTED FUTURE WORK

1. The composition of the material could be varied such that a larger amount of liquid phase is formed. This should help densify the material more.

2. Although HPC yielded satisfactory results, other plasticizers, such as HPC having a lower (100,000) or higher (1,000,000) molecular weight, could be investigated in an attempt to better understand the role of polymer/whisker interaction.

3. The effect of varying the plasticizer content could be studied in more depth, as this is also a determining factor in achieving a paste with good extrusion characteristics. Viscosity measurements on the paste could also be carried out.

4. A pugging mill could be used to produce a continuous pore-free extrudate suitable for analysis of mechanical properties. However care must be taken as prolonged exposure of the paste in a vacuum would dry up the water on the surface. This could prove to be a problem.

5. A more complete study of the strength of the material could be carried out once good extrudate can be obtained. This would probably require the setting up of a scaled down model of a semi-continuous extrusion process, where variables could be controlled more closely.

8. REFERENCES

- 1) E.J. Kubel, *Advanced Materials & Processing*, 9, (1989), 55-60.
- 2) L.M. Sheppard, *Am. Ceram. Soc. Bull.*, 68, 9, (1989), 1624-1633.
- 3) F.F. Lange, *J. Am. Ceram. Soc.*, 72, 1, (1989), 3-15.
- 4) E.J. Kubel, *Advanced Materials & Processing*, 8, (1988), 25-33.
- 5) T.J. Reinhart, in *Composites, Engineering Materials Handbook, Vol.1*, ASM Handbook, 1987, 1-40.
- 6) W.L. Lachmann in *Composites, Engineering Materials Handbook, Vol.1*, ASM Handbook, 1987, 845-903.
- 7) RILEM Symposium, *Testing and Test Methods of Fibre Cement Composites*, Edited by R.N. Swamy, The Construction Press, 1978.
- 8) E. Fitzner, D. Kehr and M. Sahebkar, *Chem. Ing. Technik*, 21, (1973), 1244-50.
- 9) S. Yajima, K. Okamura, J. Hayashi and M. Omori, *J. Am. Ceram. Soc.*, 59, 7-8, (1976) 324-27.
- 10) Y. Abe, S. Horikiri, F. Fujimura and E. Ichiki, *Proc. of the 4th Int. Conf. on Composite Materials*, Edited by Hayashi et al. ICCM IV, Tokyo, 1982.
- 11) D.P. Stinton, A.J. Caputo and R.A. Lowden, *Am. Ceram. Soc. Bull.*, 65, 2, (1986), 347-350.
- 12) R. Colmet, I. Lhermitte-Sebire and R. Naslain, *Advanced Ceramic Materials*, 1, 2, (1986), 185-91.
- 13) R.T. Bhatt, NASA Tech. Memo. No. 87085, 1985.

- 14) K. Prewo and J. Brennan, *J. Mater. Sci.*, 15, 2, (1980), 463-68.
- 15) J.A. Cornie, Y. Chaing, D.R. Uhlmann, A. Mortensen and J.M. Collins, *Am. Ceram. Soc. Bull.*, 65, 2, (1986), 293-304.
- 16) S.C. Danforth, *Proc. of the 28th Annu. Conf. Metall. of the C.I.M.*, 17, 1989, 107-119.
- 17) L.J. Schoiler and J.J. Stiglich, *Am. Ceram. Soc. Bull.*, 65, 2, (1986), 289-292.
- 18) T. Mah, M.G. Mendiratta, A.P. Katz and K.S. Mazdidasni, *Am. Ceram. Soc. Bull.*, 66, 2, (1987), 304-308.
- 19) S. Buljan, A.E. Pasto and H.J. Kim, *Am. Ceram. Soc. Bull.*, 68, 2, (1989), 387-394.
- 20) D.B. Marshall and J.E. Ritter, *Am. Ceram. Soc. Bull.*, 66, 2, (1987), 309-317.
- 21) R.W. Rice, *Am. Ceram. Soc. Bull.*, 63, 2, (1984), 256-262.
- 22) K.M. Prewo, *Am. Ceram. Soc. Bull.*, 68, 2, (1989), 395-400.
- 23) H.M. Jennings, *J. Mater. Sci.*, 18, (1983), 951-967.
- 24) E.T. Turkdogan and V.A. Tippett, *J. App. Chem.*, 8, (1958), 296.
- 25) D. Hardie and K.H. Jack, *Nature*, 179, (1957), 332.
- 26) S. Wild, P. Grieveson and K.H. Jack, *Metall. Chem. Proc. Symp.*, Edited by O. Kubaschewski, 1971, 339.
- 27) K. Kijima, K. Kato, Z. Inoue and H. Tanaka, *J. Mater. Sci.*, 10, (1975), 362.
- 28) H.F. Priest, F.C. Burns, G.L. Priest and E.C. Skaar, *J. Am. Ceram. Soc.*, 56, (1973), 395.
- 29) A.J. Edwards, D.P. Elias, M.W. Lindley, A. Atkinson and A.J. Moulson, *J. Mater. Sci.*, 9, (1974), 516.

- 30) S.N. Ruddlesden and P. Popper, *Acta Cryst.*, 11, (1958), 465.
- 31) F.L. Riley, *Nitrogen Ceramics*, (1977), 593.
- 32) D.R. Messier, F.L. Riley and R.J. Brooks, *J. Mater. Sci.*, 13, (1978), 1199.
- 33) L. Pauling in *Nature of the Chemical Bond*, 3rd edition, Cambridge Univ. Press, N.Y., 1960, 98.
- 34) G. Ziegler, J. Heinrich and G. Wotting, *J. Mater. Sci.*, 22, (1987), 3041-3086.
- 35) W.D. Kingery, H.K. Bowen and D.R. Uhlmann in *Introduction to Ceramics*, J. Wiley & Sons, N.Y., 1976.
- 36) W.D. Kingery, *J. Appl. Phys.*, 30, (1959), 301.
- 37) F. Thrummler and W. Thomas, *Int. Metall. Rev.*, 1, (1967), 69.
- 38) B.J. Weunsch and T. Vasilos. Final report 1973-75, contract no. NR032-537/8-18-72, 471. office of Naval Research, Washington D.C.
- 39) A.W.J.M. Rae, D.P. Thompson and K.H. Jack, *Proc. Army Materials Tech. Conf.*, Ceramics for High Performance Applic. II (Brook Hill), 1978, 1039.
- 40) L.J. Gauckler, Hohnke, and T.Y. Tien, *J. Am. Ceram. Soc.*, 63, (1980), 35.
- 41) K.H. Jack and W.I. Wilson, *Nature*, 238, (1972), 28.
- 42) Y. Oyama and J. Kamigaito, Japan, *J. Appl. Phys.*, 10, (1971), 1637.
- 43) P. Drew and M.H. Lewis, *J. Mater. Sci.*, 9, (1974), 261.
- 44) S.M. Boyer and A.J. Moulson, *J. Mater. Sci.*, 13, (1978), 1637.
- 45) W. Kaiser and C.D. Thurmond, *J. Appl. Phys.*, 30, (1959), 427.
- 46) K. Blegan, *Special Ceramics 6*, Edited by P. Popper, 1975, 223.
- 47) L.J. Bowen, R.J. Weston, T.G. Carruthers, and R.J. Brook, *J. Mater. Sci.*, 13,

(1978), 341.

48) F.F. Lange, *J. Amer. Ceram. Soc.*, 62, (1979), 428.

49) M.H. Lewis, A.R. Bhatti, R.J. Lumby and B. North, *J. Mater. Sci.*, 15, (1980), 103.

50) R.J. Lumby, P. Hodgson, N.E. Cother and A. Szweda, *Proc. Int. Congr. S.A.E.* paper 850521, 1985.

51) D.A. Bonnell, T.Y. Tien and M. Ruhle, *J. Am. Ceram. Soc.*, 70, (1987), 460.

52) A.J. Moulson, *J. Mater. Sci.*, 14, (1979), 1017.

53) R.W. Rice, *Ceram. Eng. Sci. Proc.*, 2, (1981), 661-701.

54) F.F. Lange, *Phil. Mag.*, 22, (1970), 983-92.

55) A.G. Evans, *Phil. Mag.*, 26, (1972), 1327-44.

56) R.J. Kerans, R.S. Hay, N.J. Pagano and T.A. Parthasarathy, *Am. Ceram. Soc. Bull.*, 68, 2, (1989), 429-442.

57) B. Bender, D. Shadwell, C. Bulik, L. Incorvati and D. Lewis, *Am. Ceram. Soc. Bull.*, 65, 2, (1986), 363-369.

58) P.F. Becher, C. Hsueh, P. Angelini and T.N. Tiegs, *Int. Conf. Proc., Whisker- and Fiber-Toughened Ceramics*, ASM, 1988, 109.

59) R.A. J. Sambell, A. Briggs, D.C. Phillips, and D.H. Bowen, *J. Mater. Sci.*, 7, (1972), 676-681.

60) E. Fitzner and R. Gadow, *Am. Ceram. Soc. Bull.*, 65, 2, (1986), 326-35.

61) D.K. Shelty, M.R. Pascucci, B.C. Mutsuddy and R.R. Wills, *Ceram. Eng. Sci. Proc.*, 7-8, (1985), 632-645.

62) C.A. Andersson, P. Barron-Antolin, A.S. Fareed and G.H. Schiroky, *Int. Conf. Proc.*,

Whisker- and Fiber-Toughened Ceramics, ASM, 1988, 209.

63) R.N. Singh and M.K. Brun, *Advanced Ceramic Materials*, 3, 3, (1988), 235-237.

64) T.N. Tieggs and P.F. Becher, *Am. Ceram. Soc. Bull.*, 66, 2, (1987), 339-42.

65) K.W. Lee and S.W. Sheargold, *Ceram. Eng. Sci. Proc.*, 10, 7-8, (1989), 702-711.

66) T. Tieggs, *Ceram. Eng. Sci. Proc.*, 10, 9-10, (1989), 1101-1107.

67) H. Lee and M.D. Sacks. *Ceram. Eng. Sci. Proc.*, 10, 7-8, (1989), 720-729.

68) J.V. Milewski, *Advanced Ceramic Materials*, 1, 1, (1986), 36-41.

69) R. Lundberg, L. Kahlman, R. Pompe, R. Carisson and R. Warren, *Am. Ceram. Soc. Bull.*, 66, 2, (1987), 330-33.

70) G. Pezzotti, I. Tanaka, T. Okamoto, Y. Miyamoto and M. Koizumi, *Ceram. Eng. Sci. Proc.*, 10, 7-8, (1989), 1015-1020.

71) F.F. Lange and M. Metcalf, *J. Am. Ceram. Soc.*, 66, 6, (1985), 398-406.

72) B.H. Lavenda, *Scientific American*, Feb. 1985, 70-85.

73) C.S. Hirtzel and R. Rajagopalan in *Colloidal Phenomena: Advanced Topic*, Noyes Publ., N.Y., 1985, 15-69.

74) J.T.G. Overbeek, *J. Coll. & Int. Sci.*, 58, 2, (1977), 408-422.

75) P.D. Shalek, J.J. Petrovic, G.F. Hurley and F.D. Gac, *Am. Ceram. Soc. Bull.*, 65, 2, (1986), 351-56.

76) H. Kodama and T. Miyoshi, *Ceram. Eng. Sci. Proc.*, 10, 9-10, (1989), 1072-1082.

77) K.G. Nickel, M.J. Hoffmann, P. Greil, and G. Petzow, *Advanced Ceramic Materials*, 3, 6, (1988), 557-62.

78) L. Zarnon, M.D. Pugh and R.A.L. Drew, *J. Am. Ceram. Soc.*, 72, 3, (1989), 495-98.

- 79) D.E. Wittmer, *Ceram. Eng. Sci. Proc.*, 9, 7-8, (1988), 735-740.
- 80) M.N. Rahaman, Y. Boiteux and L.C. De Jonghe, *Am. Ceram. Soc. Bull.*, 65, 8, (1986), 1171-76.
- 81) P.K. Whitman and D.L. Feke, *Advanced Ceramic Materials*, 1, 4, (1986), 366-70.
- 82) J.H. Adair, B.C. Mutsuddy and E.J. Drauglis, *Advanced Ceramic Materials*, 3, 3, (1988), 231-34.
- 83) M.D. Sacks, H. Lee and O.E. Rojas, *J. Am. Ceram. Soc.*, 71, 5, (1988), 370-79.
- 84) J. Homeny, W.L. Vaughn and M.K. Ferber, *Am. Ceram. Soc. Bull.*, 66, 2, (1987), 333-338.
- 85) M.J. Hoffmann, A. Nagel, P. Greil and G. Petzow, *J. Am. Ceram. Soc.*, 72, 5, (1989), 765-69.
- 86) J.R. Porter, F.F. Lange and A.H. Chokshi, *Am. Ceram. Soc. Bull.*, 66, 2, (1987), 343-347.
- 87) T. Kandori, Y. Ukyo and S. Wada, *Int. Conf. Proc., Whisker- and Fiber-Toughened Ceramics*, ASM, 1988, 125.
- 88) C.W. Griffin, A.C. Hurford, A.V. Virkar and D.W. Richardson, *Ceram. Eng. Sci. Proc.*, 10, 7-8, (1989), 695-706.
- 89) P.F. Becher and T.N. Tiegs, *Advanced Ceramic Materials*, 3, 2, (1988), 148-53.
- 90) S.T. Buljan, J.G. Baldoni and M.L. Huckabee, *Am. Ceram. Soc. Bull.*, 66, 2, (1987), 347-52.
- 91) L.J. Neergaard and J. Homeny, *Ceram. Eng. Sci. Proc.*, 10, 9-10, (1989), 1049-1062.
- 92) N.D. Corbin, C.A. Willkens, V.K. Pujari, R.L. Yeckley and M.J. Mangaudis, *Int.*

- Conf. Proc., Whisker- and Fiber-Toughened Ceramics, ASM, 1988, 131.*
- 93) T.N. Tiegs, *Int. Conf. Proc., Whisker- and Fiber-Toughened Ceramics, ASM, 1988, 105.*
- 94) A. Lightfoot, B.W. Sheldon, J.H. Flint and J.S. Haggerty, *Ceram. Eng. Sci. Proc., 10, 9-10, (1989), 1035-1048.*
- 95) C.J. Shih, J. Yang and A. Ezis, *Ceram. Eng. Sci. Proc., 10, 9-10, (1989), 1064-1071.*
- 96) P.F. Becher and T.N. Tiegs, in *Composites, Engineering Materials Handbook, Vol.1, ASM Handbook, 1987, 941-944.*
- 97) M. Yamamoto, T. Kida and K. Sugihara, *Int. Conf. Proc., Whisker- and Fiber-Toughened Ceramics, ASM, 1988, 73-75.*
- 98) J.F. Porter, *Int. Conf. Proc., Whisker- and Fiber-Toughened Ceramics, ASM, 1988, 147.*
- 99) M.D. Pugh and R.A.L. Drew, *J. Can. Ceram. Soc., 58, 2, (1989), 45-49.*
- 100) R.S. Werbowyj and D.C. Gray, *Macromolecules, 13, (1980), 69-73.*
- 101) S. Fortin and G. Charlet, *Macromolecules, 22, (1989), 2286-2292.*
- 102) ASTM C373-72, "Standard Test Method for Water Absorption, Bulk Density, Apparent Porosity and Apparent Specific Gravity of Fired Whiteware Products".
- 103) M.T. Laugier, *J. Mater. Sci. Letters, 6, (1987), 355-56.*
- 104) Flexural Strength of High Performance Ceramics at Ambient Temperature, MIL-STD-1942(MR) 21 Nov. 1983, 8.
- 105) B.R. Lawn, A.G. Evans and D.B. Marshall, *J. Am. Ceram. Soc., 63, (1980), 574.*
- 106) R.W. Rice, K.R. McKinney, C.C. Wu, S.W. Freiman and W.J.M. Donough, *J. Mater.*

Sci., 20, (1985), 1392-1406.

107) K. Matsuhira and T. Takahashi, *Ceram. Eng. Sci. Proc.*, 10, 7-8, (1989), 807-816.

108) I. Tsao, S.C. Danforth and A.B. Metzner, *Proc. 28th Annu. Conf. Metall. of the C.I.M.*, Halifax, N.S., 17, 1989, 27-29.

109) C. Hyde, in *Ceramic Fabrication Processes*, Edited by W.D. Kingery, M.I.T. Press, Cambridge, Mass., 1967.

110) A.R. Teter, *Ceram. Age*, 82, 8, (1966), 30-32.

111) D.C. Gray, Personal Communication, McGill University, Montreal.

112) D.W. Richardson, in *Modern Ceramic Engineering*, M. Dekker Inc., N.Y. 1982.